CHAPTER V
RESULTS AND DISCUSSION

In this chapter, the results and discussions are divided to two sections. First, characterizations of Beta zeolites are presented in section 5.1 that is analyzed by XRD, XRF, BET surface area, SEM and FTIR pyridine adsorption. Second, catalytic behavior of Beta zeolite on the alkylation of benzene and isopropanol for cumene synthesis are explained in section 5.2.

## 5.1 Catalyst Characterization

5.1.1 X-ray Diffraction (XRD)

The catalysts prepared are analyzed by X-ray diffraction for identifying crystal structure. The X-ray diffraction patterns of H-Beta zeolite (Si/Al = 26), Na-form, NH$_4$-form, H-form of Beta zeolite (Si/Al = 41) and H-Beta zeolite (Si/Al = 70) are illustrated in Figure 5.1. The patterns of catalysts were corresponding well with those reported in the literature [8]. This indicated that all the prepared catalysts have the same structure as Beta zeolite.

5.1.2 BET Surface Area

BET surface areas of the catalysts are shown in Table 5.1. Beta zeolite in different form of Na, NH$_4$, H-form and different Si/Al ratio had BET surface area in approximately the same range.
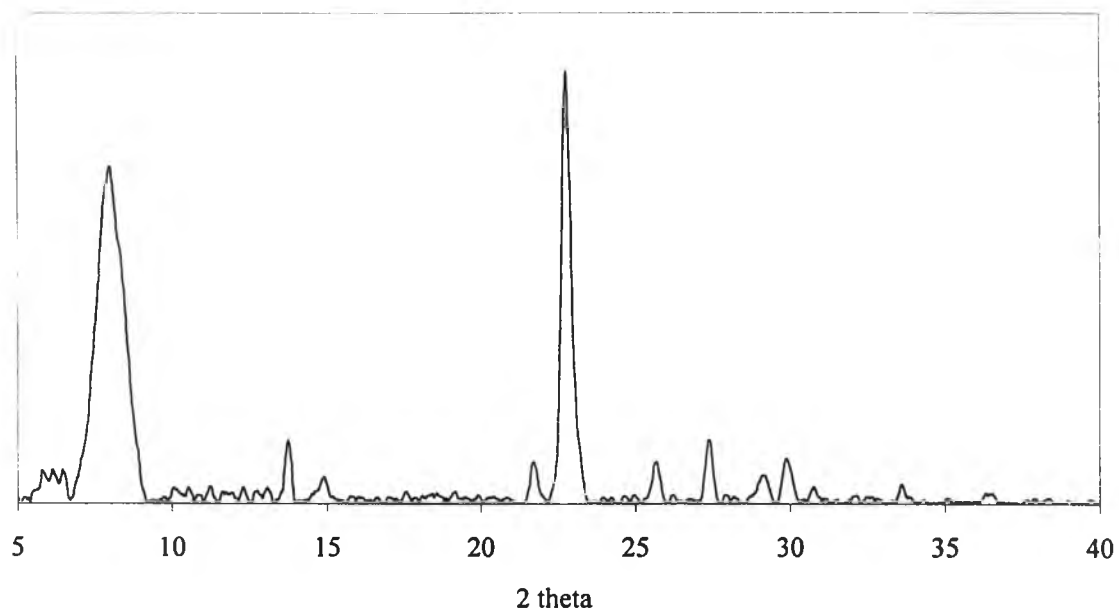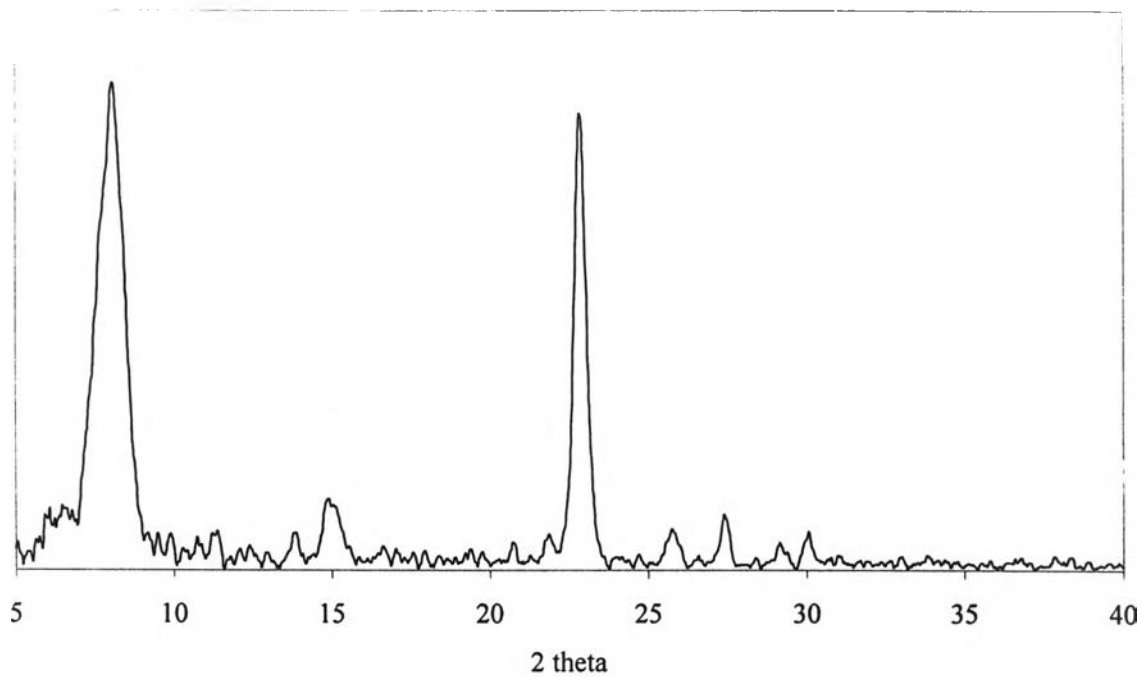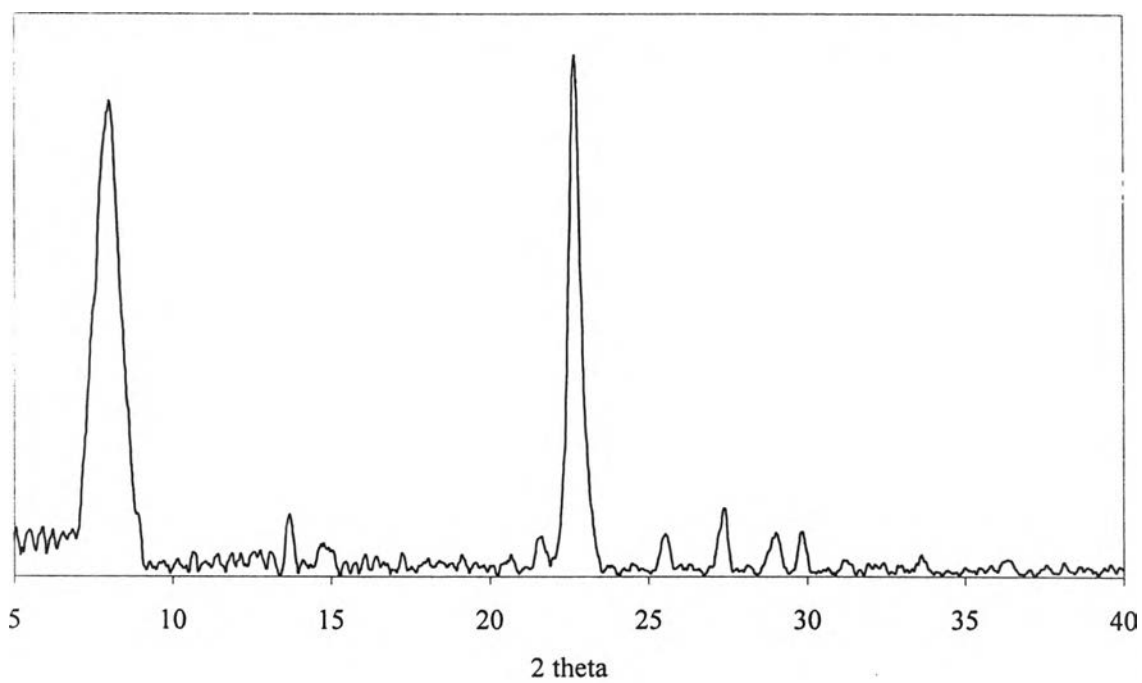
(a) H-Beta zeolite (Si/Al = 26)
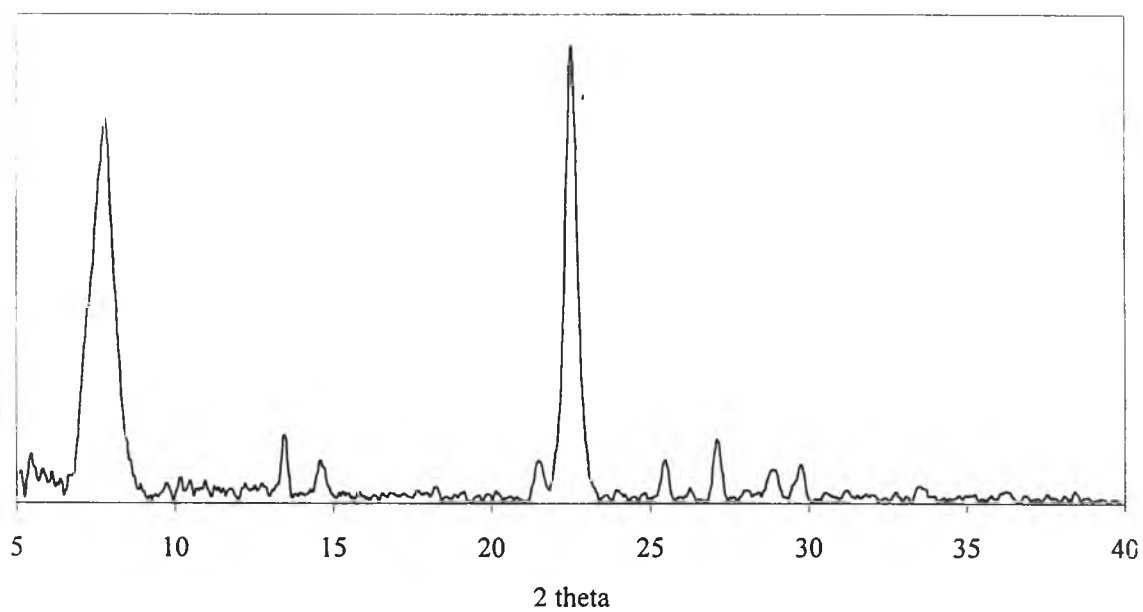
(b) Na-Beta zeolite (Si/Al = 41)

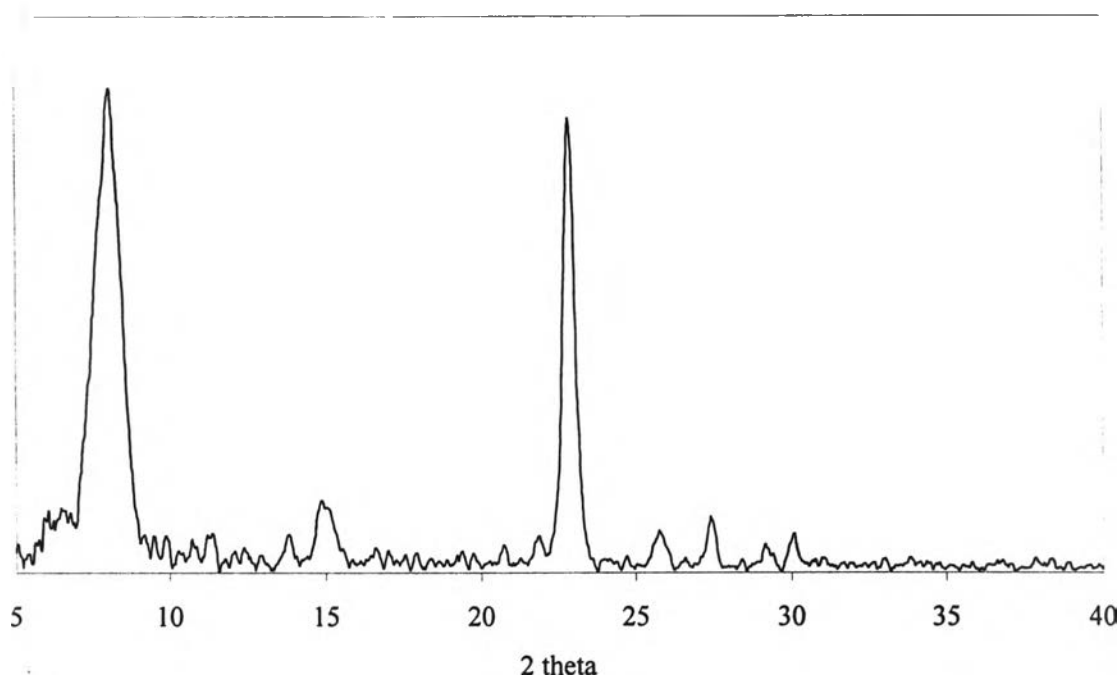**Figure 5.1** X-ray diffraction pattern of Beta zeolite

(c) NH$_4$-Beta zeolite (Si/Al = 41)

(d) H-Beta zeolite (Si/Al = 41)

Figure 5.1 X-ray diffraction pattern of Beta zeolite (continued)

(e) H-Beta zeolite (Si/Al = 70)

Figure 5.1 X-ray diffraction pattern of Beta zeolite (continued)

Table 5.1 BET surface areas of the catalysts

| Catalyst	BET surface areas (m^2/g of catalyst)
H-Beta (Si/Al = 26)	634.9
Na-Beta (Si/Al = 41)	630.8
NH₄-Beta (Si/Al = 41)	628.1
H-Beta (Si/Al = 41)	632.1
H-Beta (Si/Al = 70)	626.4

5.13 Chemical Composition

The results of quantitative analysis by XRF of silica and aluminium in the synthesized crystals are shown in table 5.2.

Table 5.2 Si/Al content in catalysts.

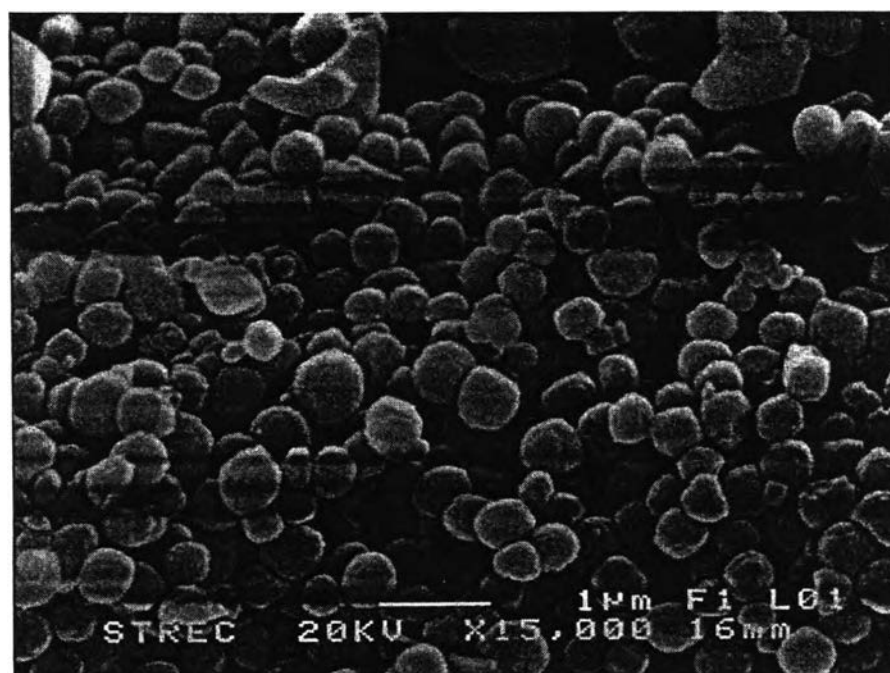| Si/Al molar ratio of H-Beta	Si/Al molar ratio observed
30	26
50	41
80	70

5.1.4 Morphology

Scaning Electron Microscope (SEM) photographs of the prepared catalysts are shown in Figure 5.2. As shown, all the catalysts were composed of roughly crystallized spherical particles.
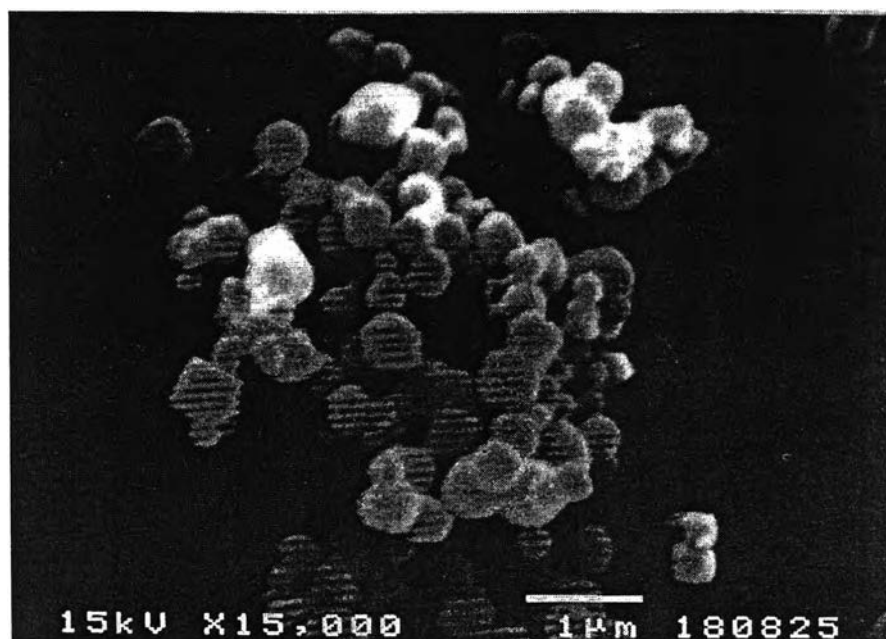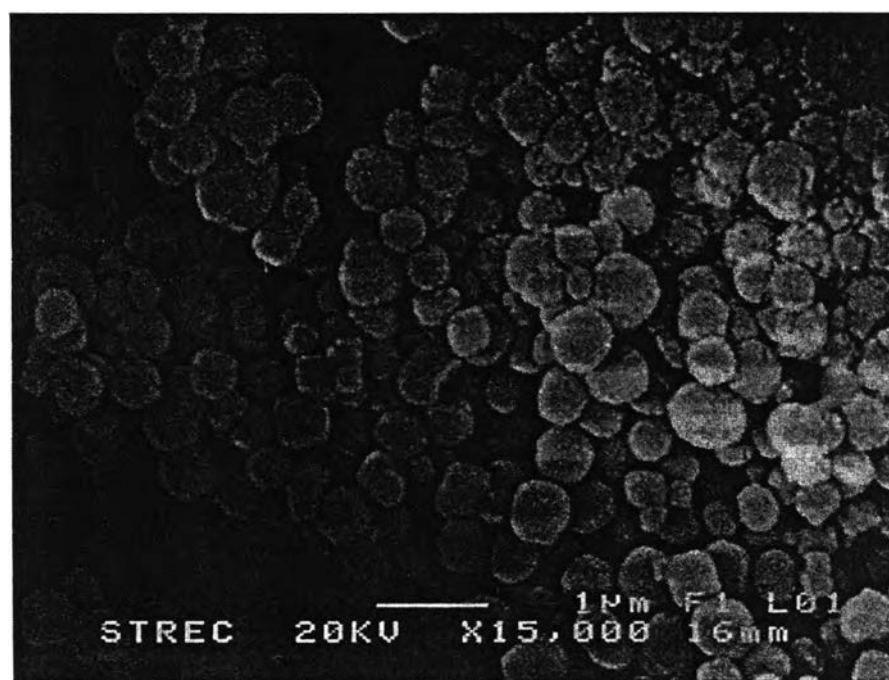

(a) H-Beta (Si/Al = 26)

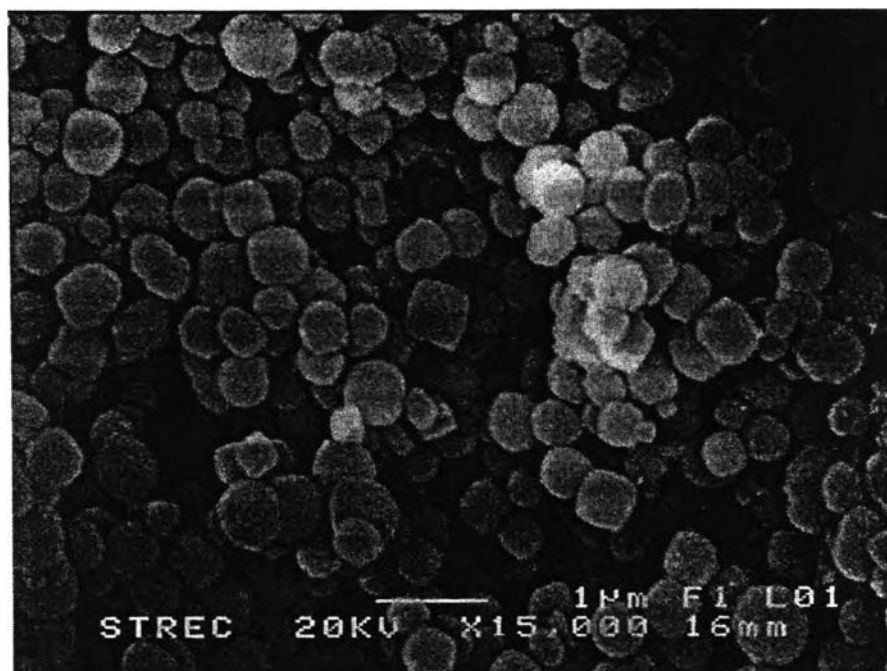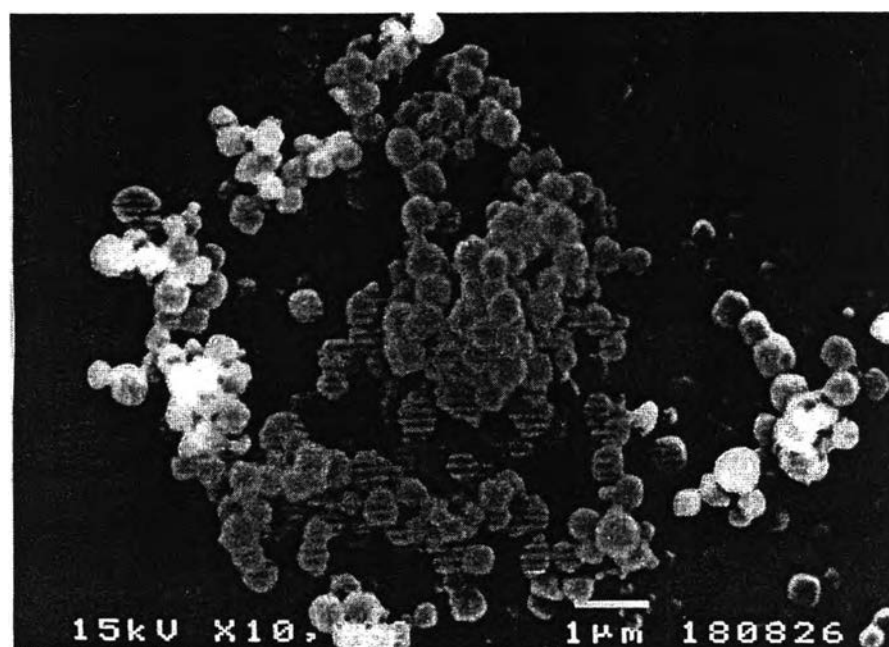**Figure 5.2** SEM photographs of catalysts

(b) Na-Beta (Si/Al = 41)

(c) NH₄-Beta (Si/Al = 41)

Figure 5.2 SEM photographs of catalysts (continued)

(d) H-Beta (Si/Al = 41)

(e) H-Beta (Si/Al = 70)

Figure 5.2 SEM photographs of catalysts (continued)

5.1.5 FTIR Pyridine Adsorption

Figure 5.3 to 5.5 illustrate the relevant region of IR spectrum after exposure'to pyridine as a function of temperature of evacuation on H-Beta (Si/Al = 26), H-Beta (Si/Al = 41) and (Si/Al = 70) respectively. Admission of pyridine resulted in the appearance of bands in the region of interest, between 1600-1400 cm^{-1}. The appearance of bands at 1540 and 1450 cm^{-1} demonstrates the presence of Brønsted and Lewis acid site respectively [37].

A number of changes are observed on evacuation when increasing temperature. After evacuation between 150°C and 500°C, a gradual reduction in the intensity of the pyridine adsorbed on both at Brønsted and Lewis sites appeared.

From Figure 5.6 to 5.8 show amount of pyridine desorbed from Lewis and Brønsted acid sites in the range of 100 – 500 °C. It has been found that the integral amounts of pyridine desorbed are decrease when Si/Al ratios increase. It has been suggested that the amount of acid sites tends to decrease with the increasing Si/Al ratio.

5.1.6 Temperature programmed oxidation

Figure 5.9 represents the temperature programmed oxidation (TPO) curves of H-Beta 26, 41 and 70. It has been found that the amount of coke (can see from CO_2 area) is increased with decreased Si/Al ratio. It had been generally accepted that coke mostly occurs on strong acid sites. Thus, the lower Si/Al ratio has the amount of strong acid sites more than the higher Si/Al ratio.
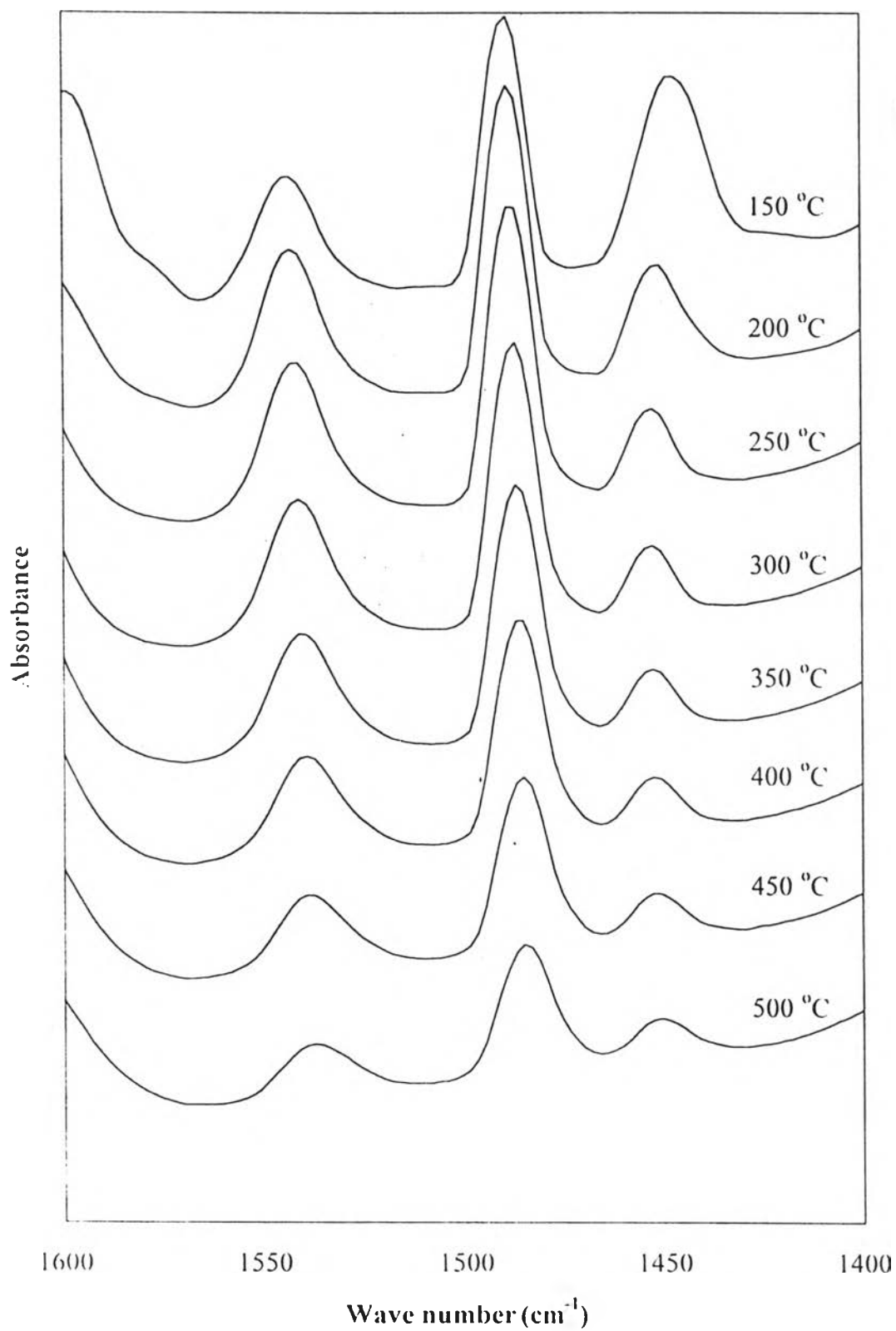
Figure 5.3   FTIR spectra of pyridine absorbed on H-Beta (Si/Al = 26)
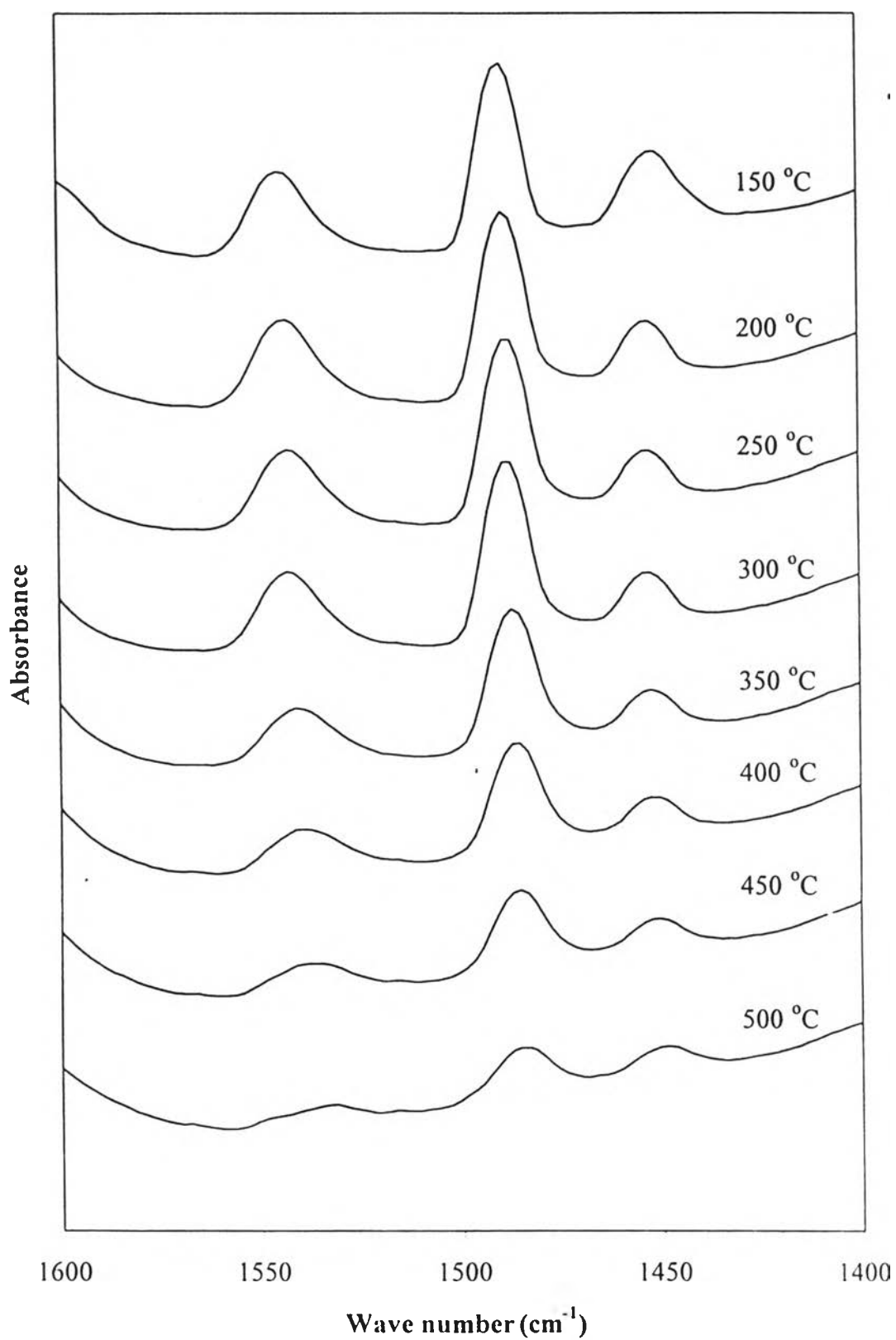
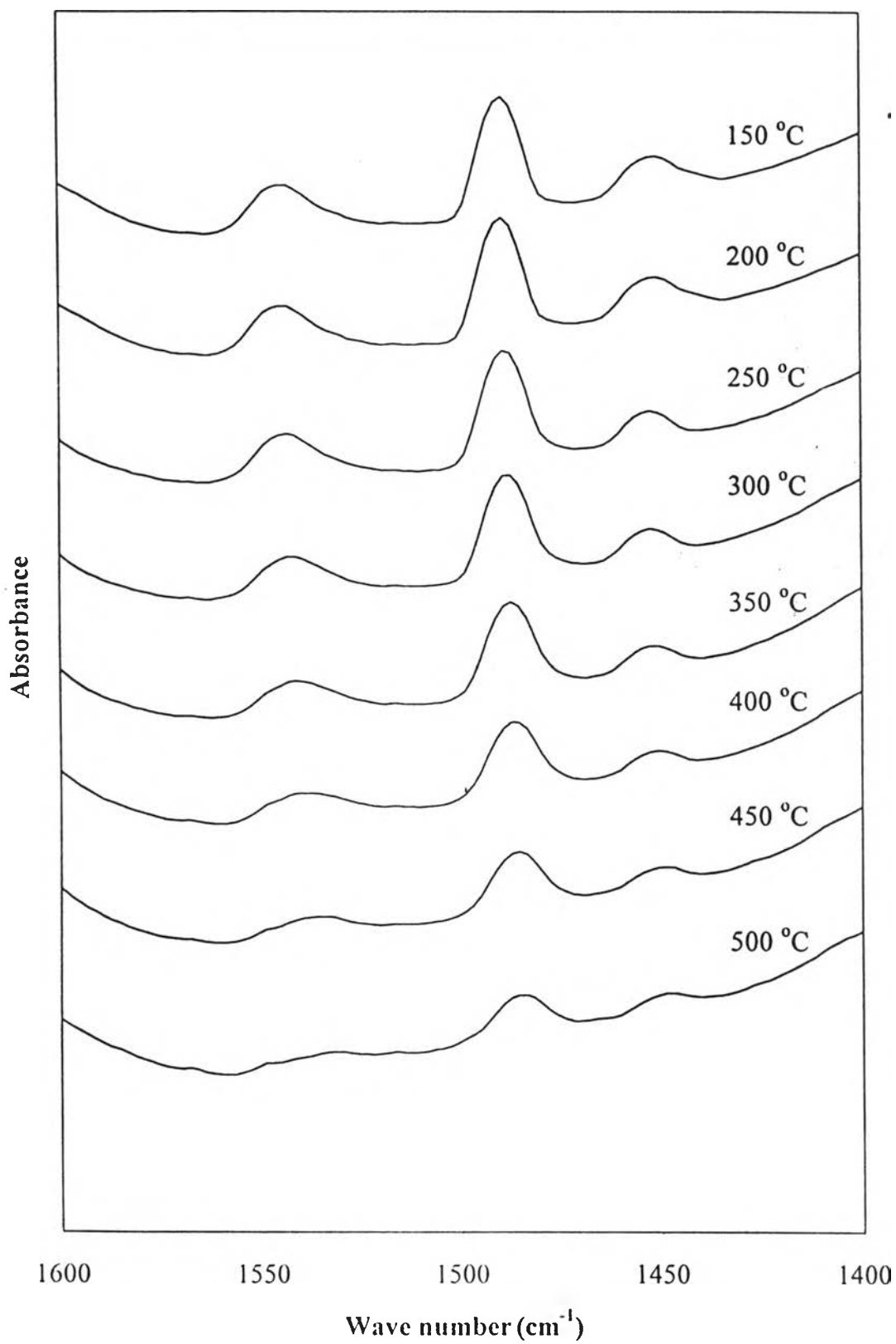**Figure 5.4** · FTIR spectra of pyridine absorbed on H-Beta (Si/Al = 41)

Figure 5.5   FTIR spectra of pyridine absorbed on H-Beta (Si/Al = 70)

Figure 5.6 The percentage of the band height of pyridine adsorbed on Lewis (A) and Brønsted (B) acid site and the amount of pyridine desorbed from Lewis (C) and Brønsted (D) acid site on H-Beta zeolite (Si/Al = 26)

Figure 5.7 The percentage of the band height of pyridine adsorbed on Lewis (A) and Brønsted (B) acid site and the amount of pyridine desorbed from Lewis (C) and Brønsted (D) acid site on H-Beta zeolite (Si/Al = 41)
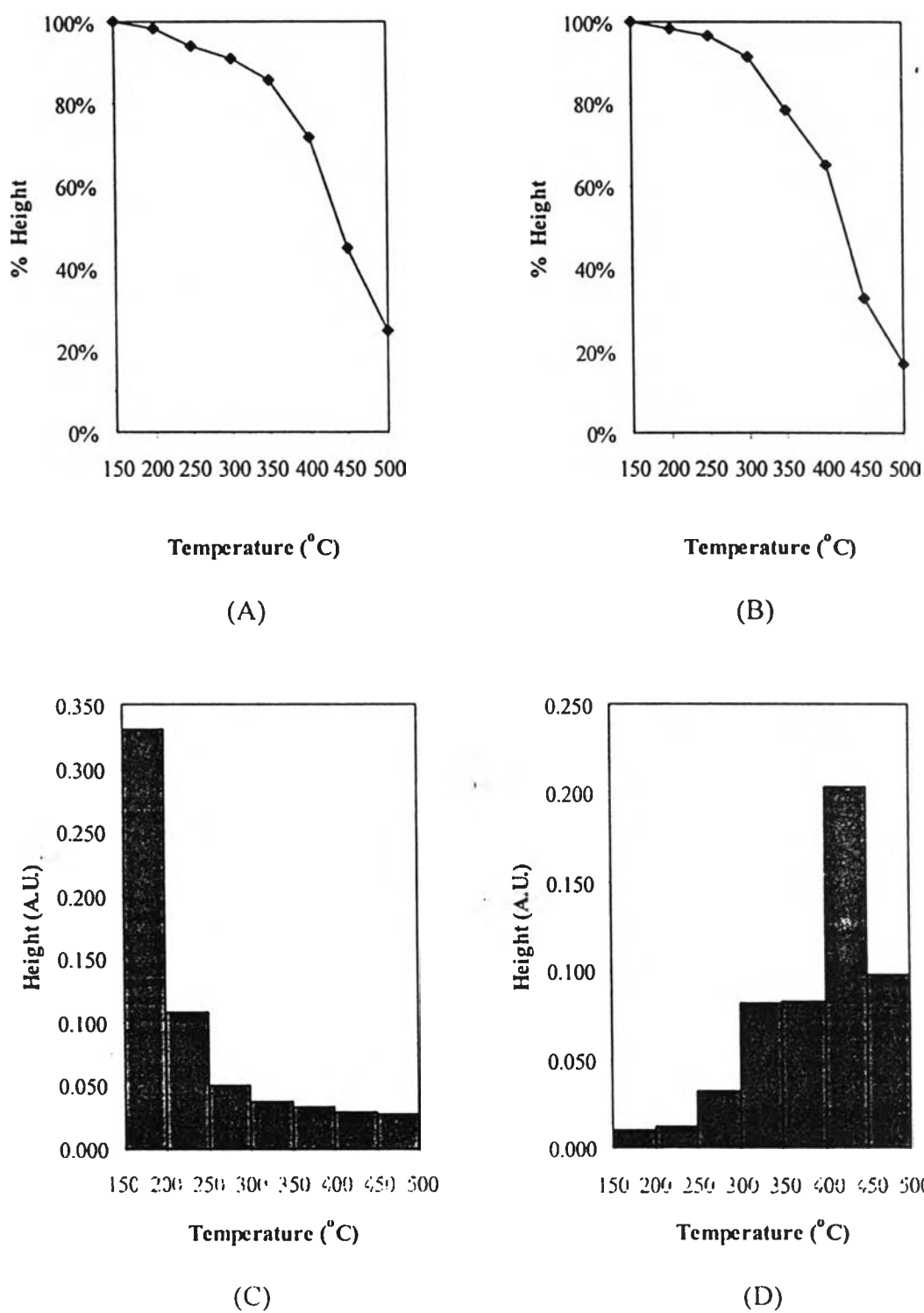
Figure 5.8   The percentage of the band height of pyridine adsorbed on Lewis (A) and Brønsted (B) acid site and the amount of pyridine desorbed from Lewis (C) and Brønsted (D) acid site on H-Beta zeolite (Si/Al = 70)
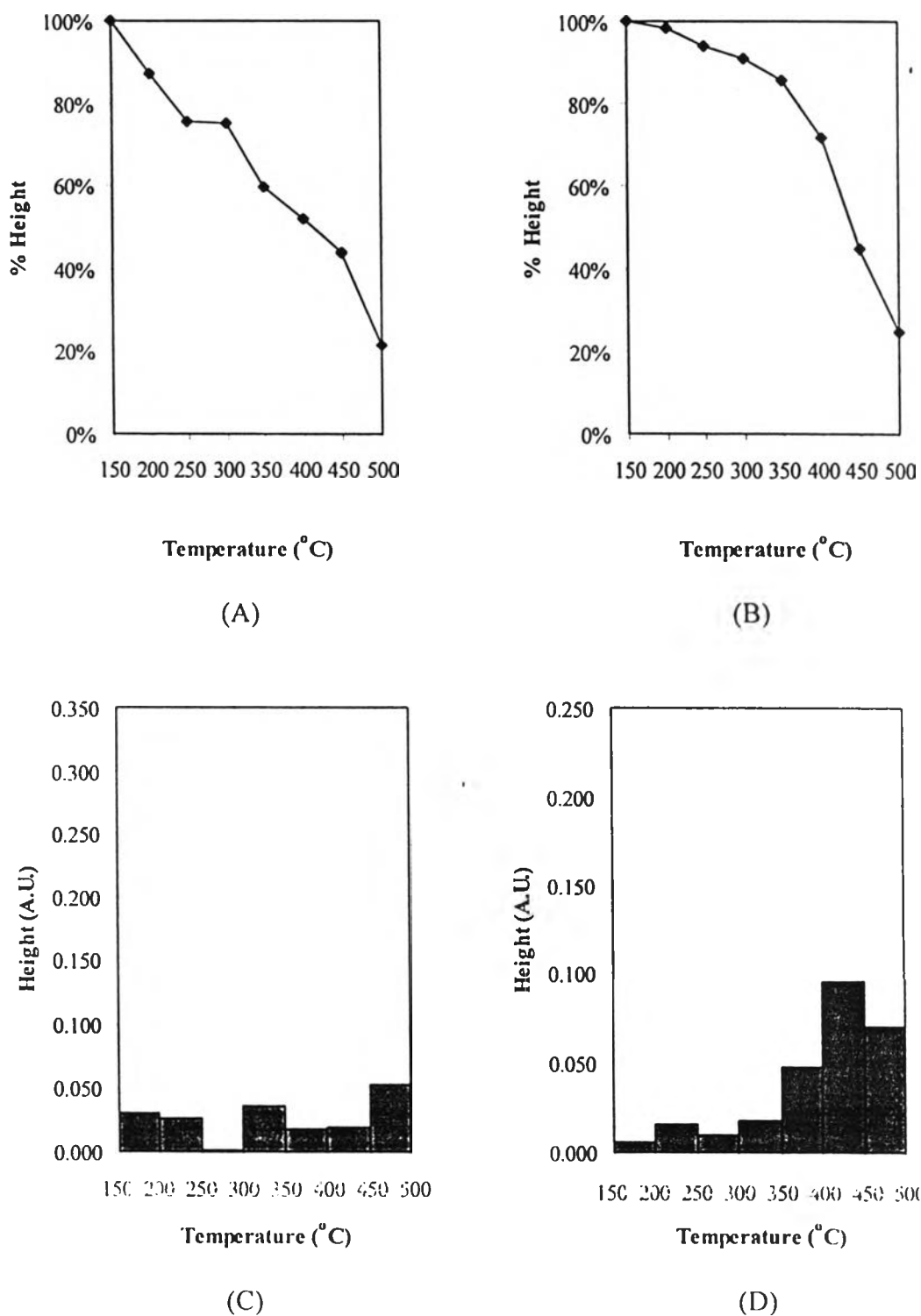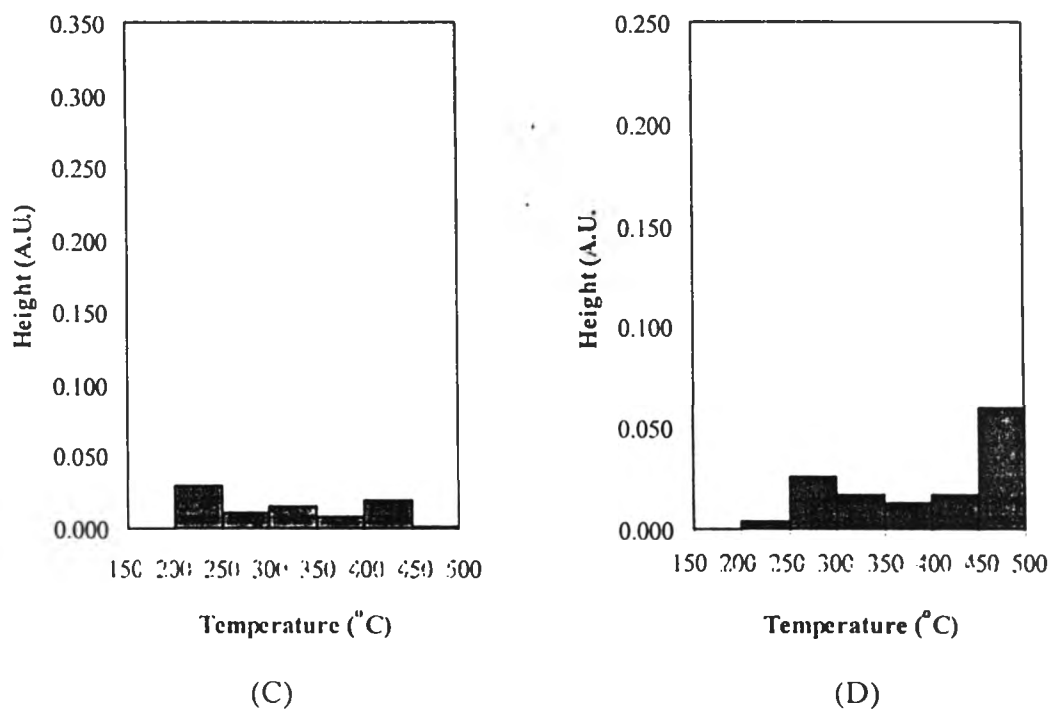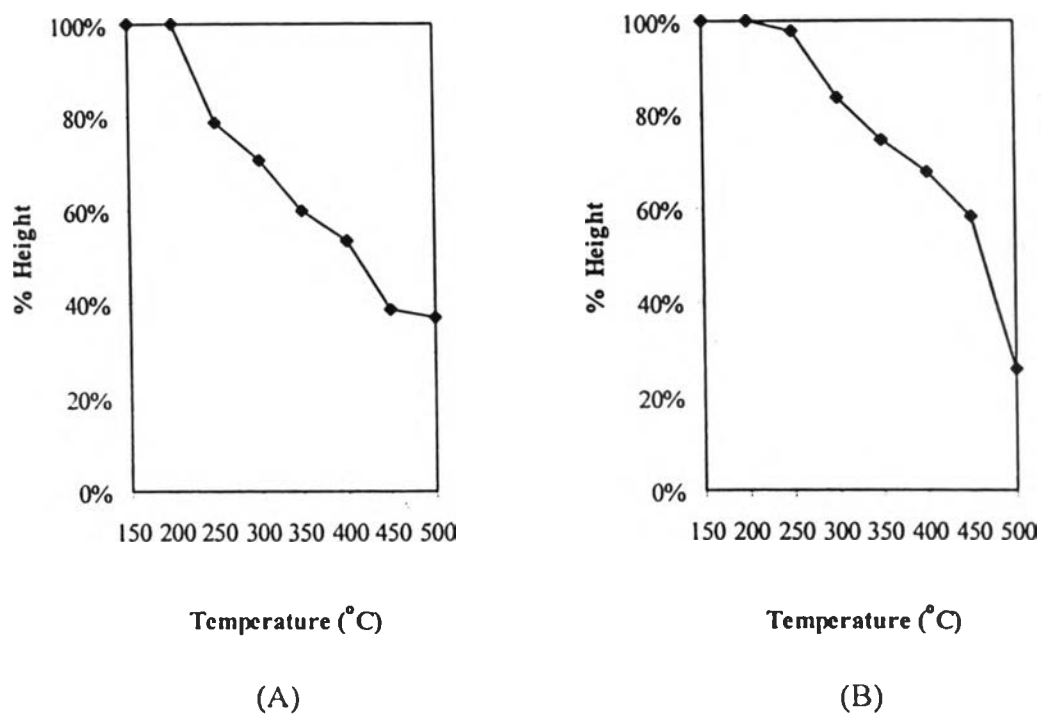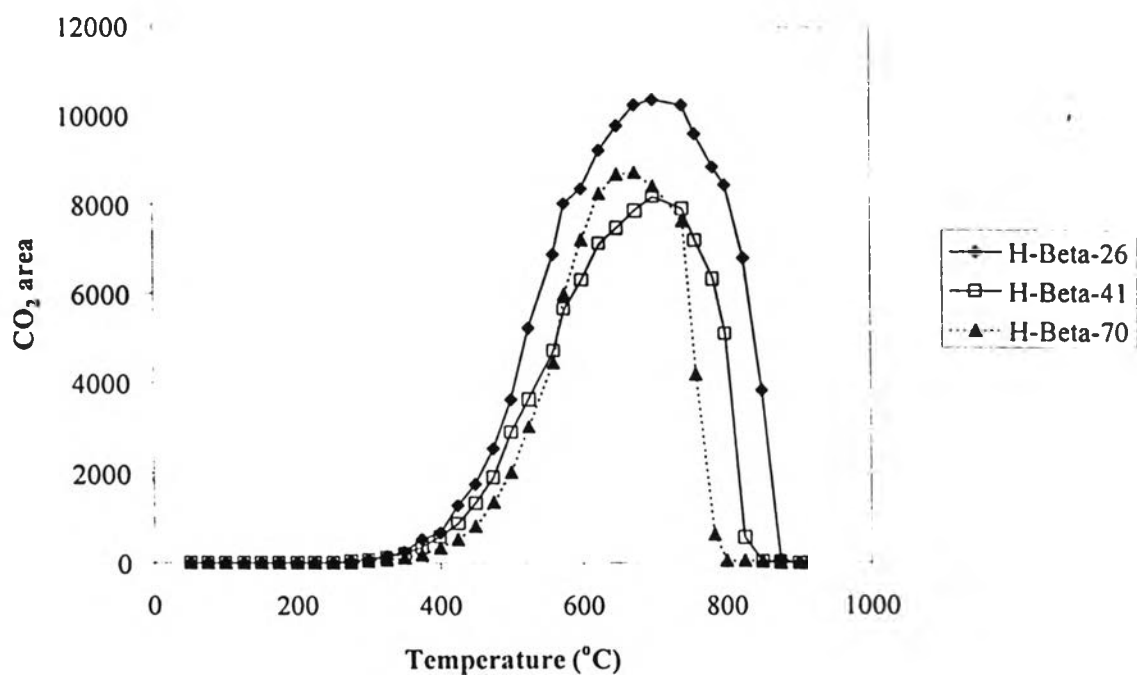
Figure 5.9 Temperature programmed oxidation of H-Beta with Si/Al ratio 26, 41 and 70

5.2 Catalytic Reaction

In this section, the catalytic properties of catalyst prepared in this research are investigated by testing the alkylation of benzene with isopropanol (benzene/isopropanol mole ratio = 2.8). The influence of different reaction parameters such as reaction temperature, gas hourly space velocity (GHSV) and Si/Al ratio were systematically studied over H-Beta zeolite.

5.2.1 The Effect of Temperature on the alkylation of benzene with isopropanol

The reaction temperatures were varied from 100 to 300°C. The reaction was carried out over H-Beta (Si/Al = 41) at GHSV 3000 h^{-1} for 40 min on stream.

The conversions of benzene and isopropanol, and selectivity for cumene are shown in Figure 5.10. Figure 5.11 represents production distribution. The conversions of benzene and selectivity for cumene are highest at 200°C. From figure 5.10, formation of Diisopropylbenzene (DIPB) decreases at high temperatures, due to the transalkylation of DIPB with benzene to cumene [33]. At the same time dealkylation of cumene also occurs at temperatures above 200°C [13]. At higher reaction temperatures, formation of side products like toluene, xylene and n-propylbenzene is also seen. Formation of these products is mainly due to the dealkylation and cracking reactions of alkybenzenes taking place at higher temperatures.

Among the DIPB, the *meta* isomer is always predominant over the *para* isomer [38]. Due to the steric hindrance the formation of *ortho* (1,2 diisopropylbenzene) isomer did not occur [39].

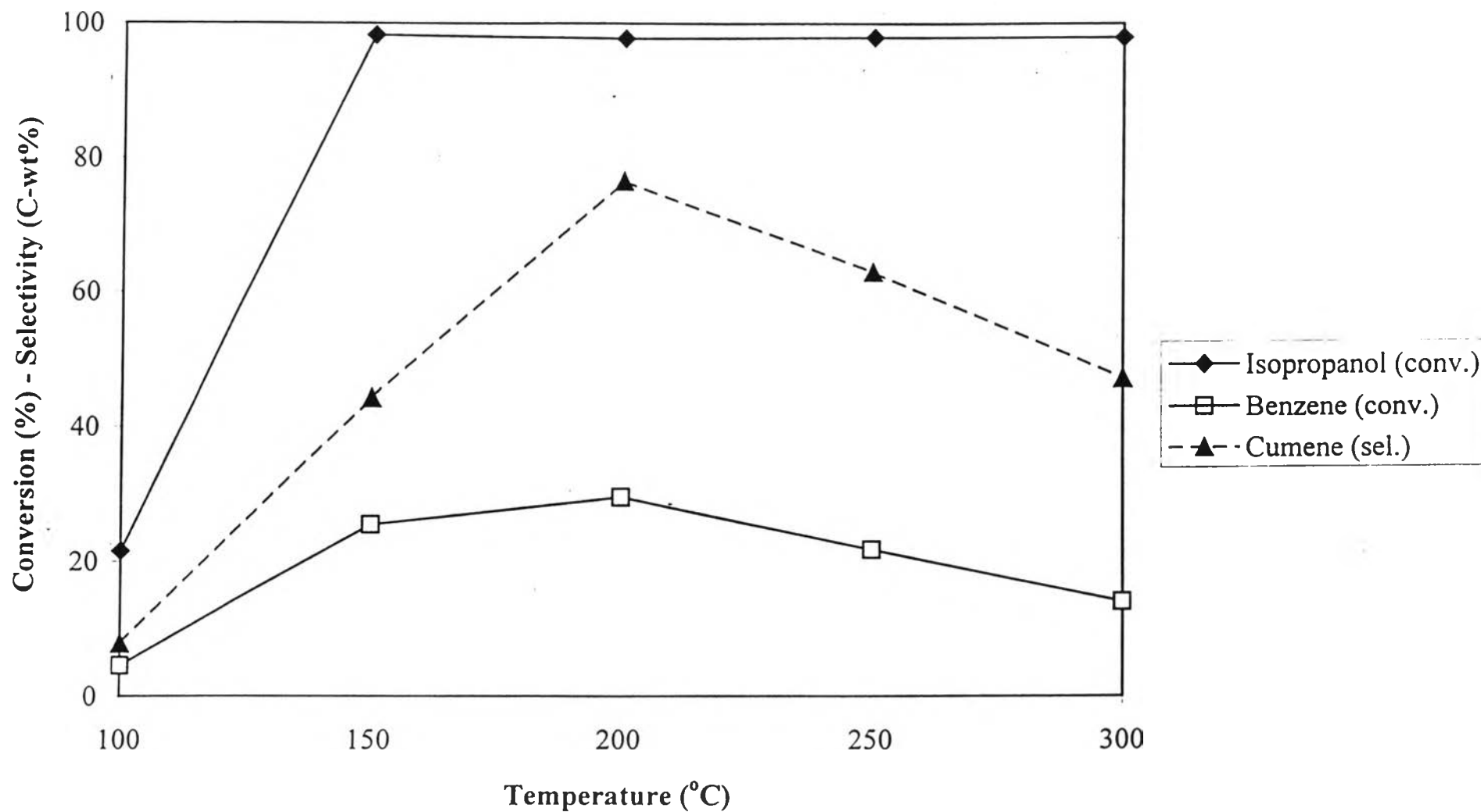**Figure 5.10** Effect of temperature on conversion and selectivity.
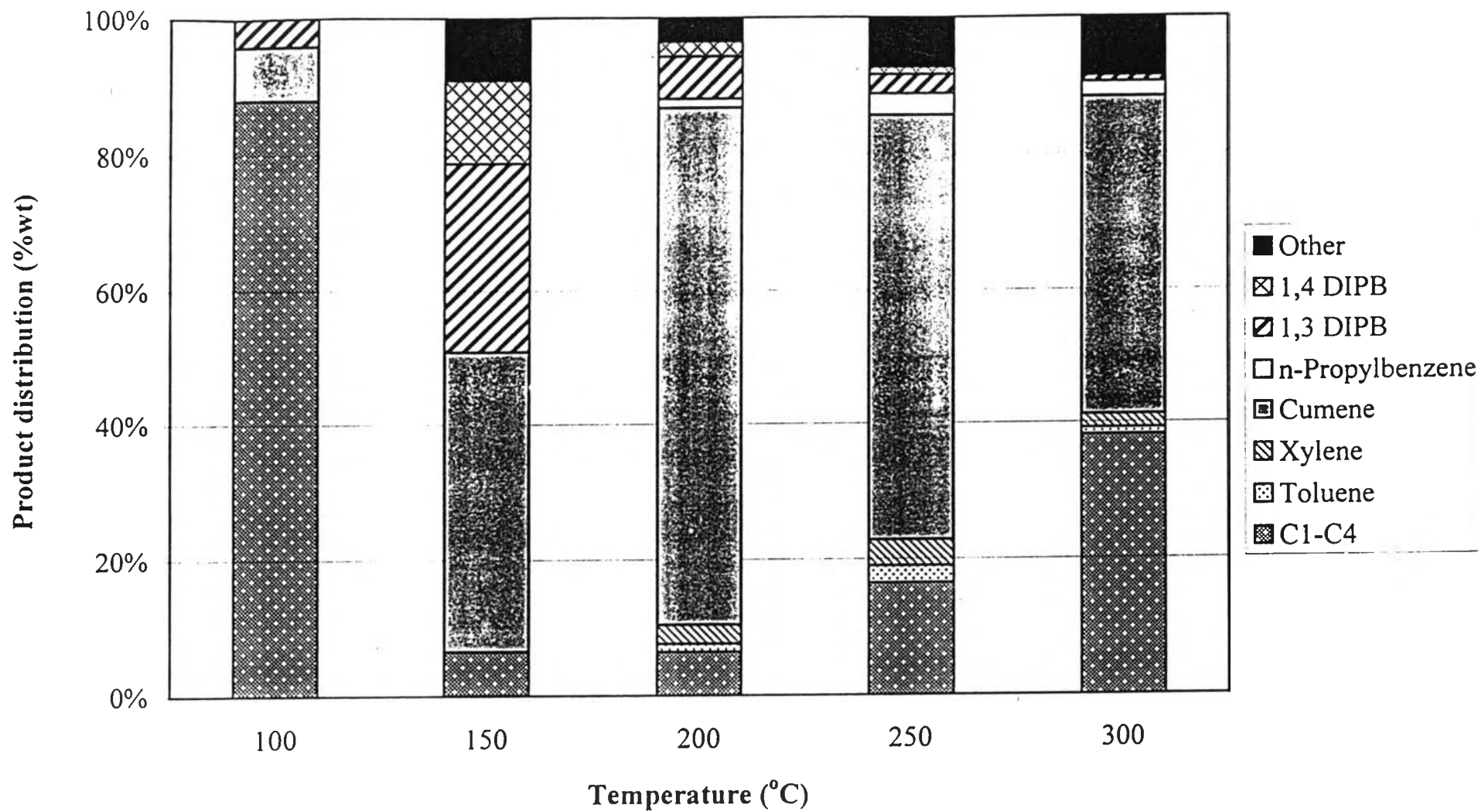Condition: GHSV 3000 h^{-1}, TOS 40 min, H-Beta Si/Al = 41.

Figure 5.11 Effect of temperature on product distribution.
Condition: GHSV 3000 h^{-1}, TOS 40 min, H-Beta Si/Al = 41.

5.2.2 The Effect of GHSV on the alkylation of benzene with isopropanol

From Figure 5.12, the conversion of benzene and isopropanol and selectivity for cumene are compared in GHSV range of 1000 to 5000 h^{-1}. Product distribution is illustrated in Figure 5.13. The reaction was carried out at temperature 200°C, TOS 40 min on H-Beta (Si/Al = 41). The relatively constant benzene and isopropanol conversion during the whole range of GHSV reflected that almost all the amount of isopropanol supplied to the reaction was reacted. The selectivity to cumene is highest at GHSV 3000 h^{-1}. The selectivity to cumene increases while GHSV decreases from 5000 to 3000 h^{-1} (higher contact time). This is because of the transalkylation of DIPB with benzene. In addition, cumene is decreased when GHSV less than 3000 h^{-1} due to the formation of dealkylation and other side reactions; consequently, the side products are increased.

5.2.3 The Effect of Time-on-stream on the alkylation of benzene with isopropanol

Figure 5.14 shows the effect of time on stream on conversion and selectivity that is investigated in the range of 10-360 minutes. The reaction was carried out at temperature 200°C, GHSV 3000 h^{-1} over H-Beta (Si/Al = 41). During this study the selectivity to cumene reaches the highest level at 40 minutes and then slightly decreases. After reaching 180 minutes, it tends to decrease slightly while DIPBs tend to increase. This is because there is deactivation of catalysts.
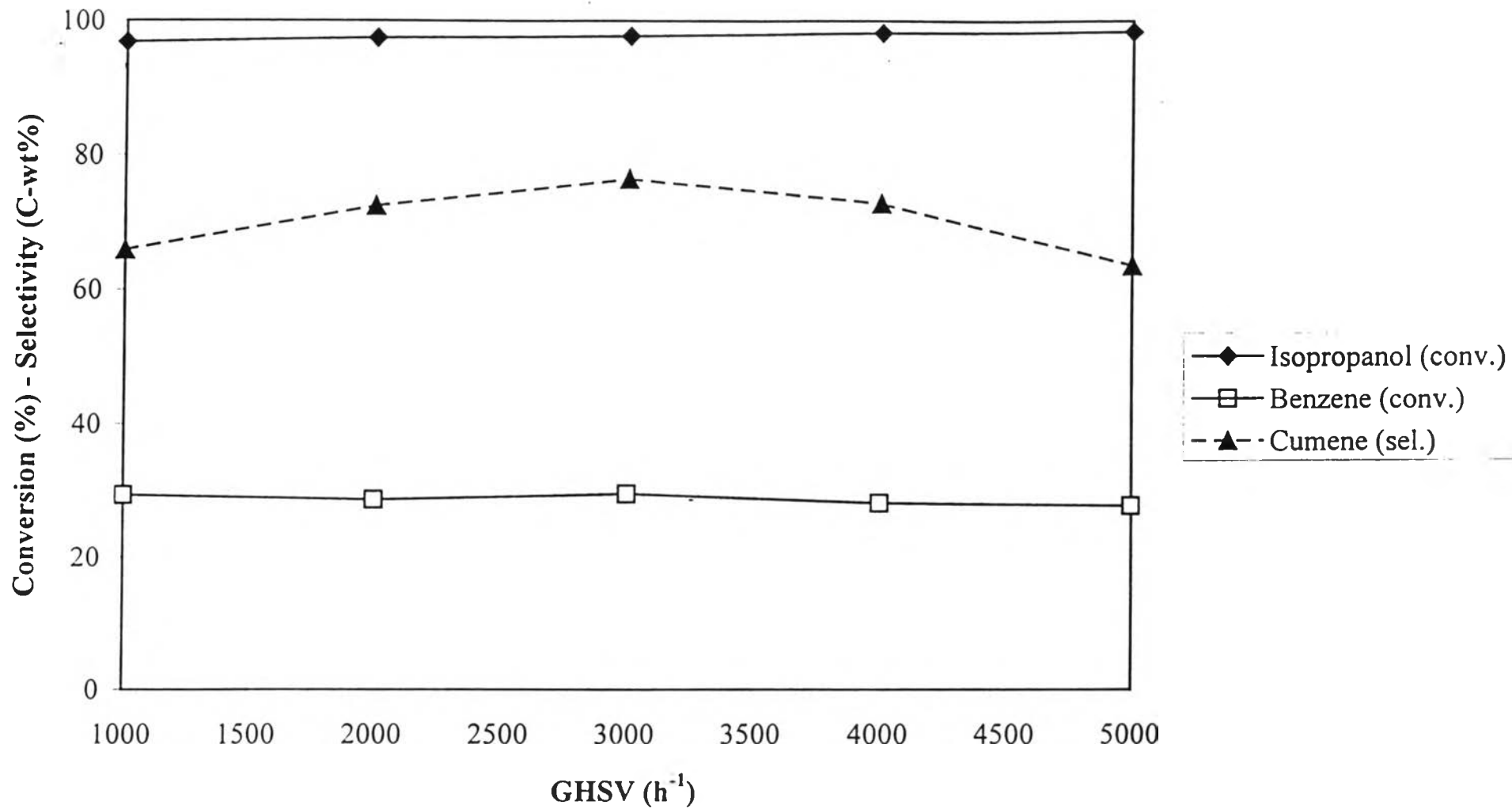
Figure 5.12 Effect of GHSV on conversion and selectivity.
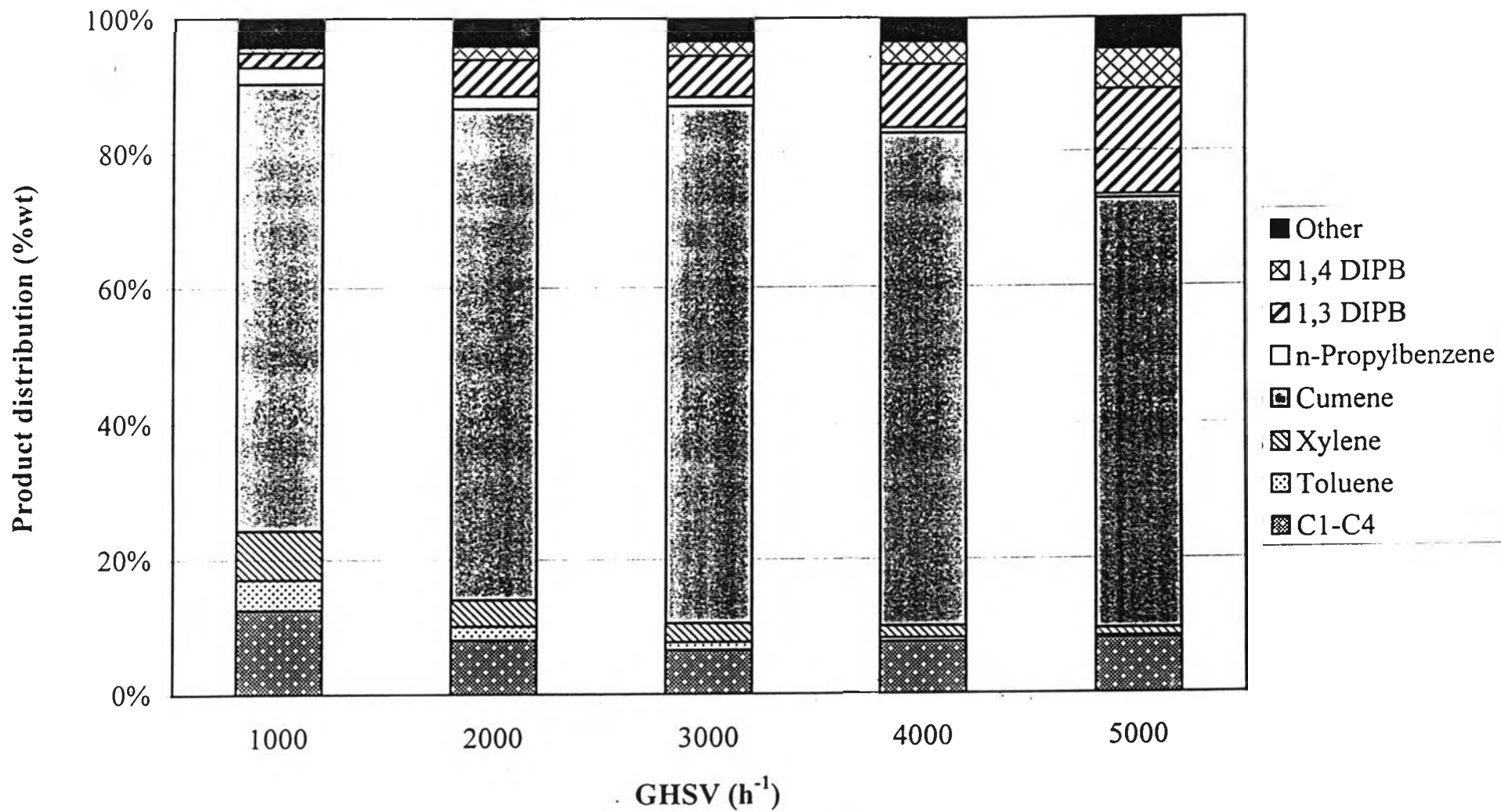Condition: Temperature 200°C, TOS 40 min, H-Beta Si/Al = 41.

Figure 5.13 Effect of GHSV on product distribution.

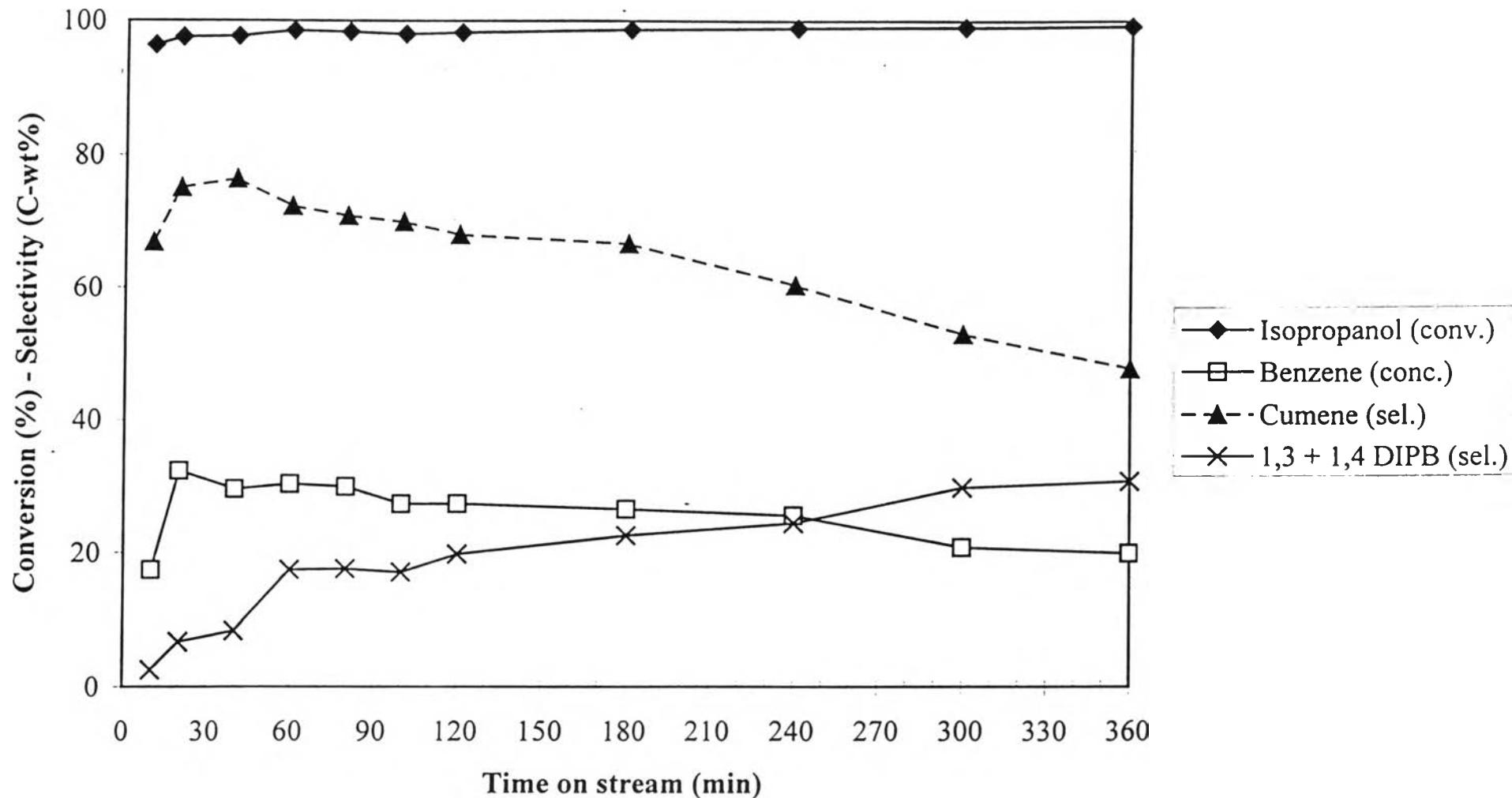Condition: Temperature 200°C, TOS 40 min, H-Beta Si/Al = 41.

Figure 5.14 Effect of time-on-stream on conversion and selectivity.

Condition: Temperature 200°C, GHSV 3000 h^{-1}, H-Beta Si/Al = 41.

5.2.4 The Effect of form of catalyst on the alkylation of benzene with isopropanol

From Figure 5.15, the conversion and selectivity are compared with using Beta zeolite in different form as the catalysts. The product distribution was shown in Figure 5.16. The reaction was carried out at 200°C, GHSV 3000 h⁻¹, TOS 40 min and Si/Al = 41. H-Beta zeolite shows higher performance than Na-form and NH₄-form. It suggested that this reaction require more acidity. The effect of acidity will be discussed in detail later.

5.2.5 The Effect of Si/Al ratios on the alkylation of benzene with isopropanol

Figure 5.17 shows the conversion of benzene and isopropanol and selectivity of cumene over H-Beta zeolite at different Si/Al molar ratios (26, 41, 70). The reaction temperature, GHSV and TOS are 200°C, 3000 h⁻¹ and 40 min, respectively. The product distribution is shown in Figure 5.18. The conversion of isopropanol in all case was more than 97% and was found to be independent of the Si/Al ratio. The conversion of benzene and the selectivity to cumene are increase when Si/Al ratios decrease. In consistent with temperature programmed oxidation, the H-Beta zeolite having higher amount of strong acid sites could be in order of H-Beta (26) > H-Beta (41) > H-Beta (70). Therefore, it has been suggested that the cumene formation is require higher strong acid sites.

The conversion of benzene and isopropanol as well as the selectivity for cumene with Si/Al ratios of 26, 41, and 70 at different times on stream are shown in Figure 5.19. It has been found that the activity of H-Beta (26) decreased faster than H-Beta (41) and H-Beta (70), respectively, due to the formation of coke on catalysts. This suggests that H-Beta (26) having the amount of acid sites more than H-Beta (41) and H-Beta (70) respectively is susceptible to coke formation on its existing acid sites.
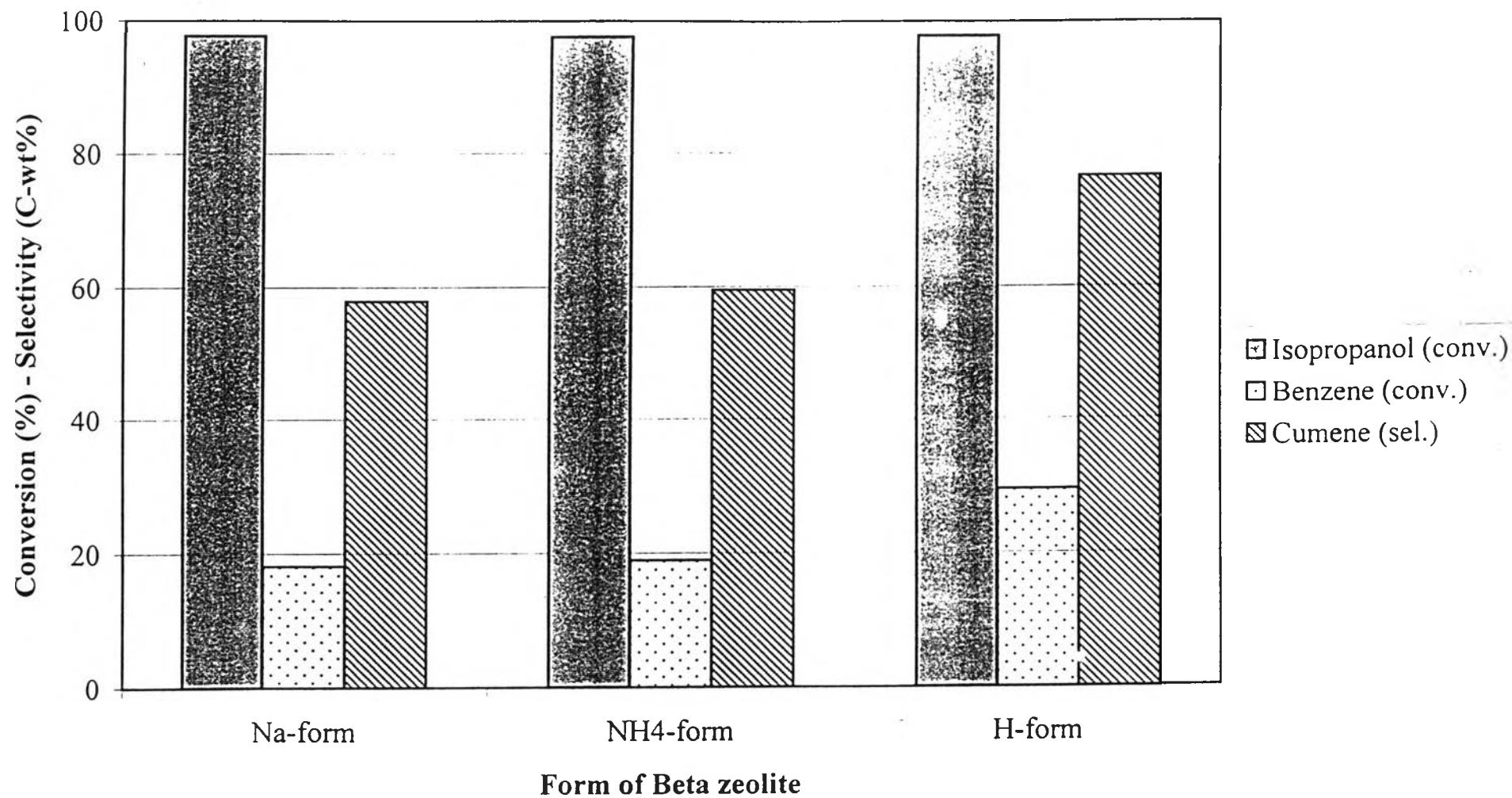
Figure 5.15 Effect of form of catalysts on conversion and selectivity.
Condition: Temperature 200°C, GHSV 3000 h^{-1}, TOS 40 min, H-Beta Si/Al = 41.
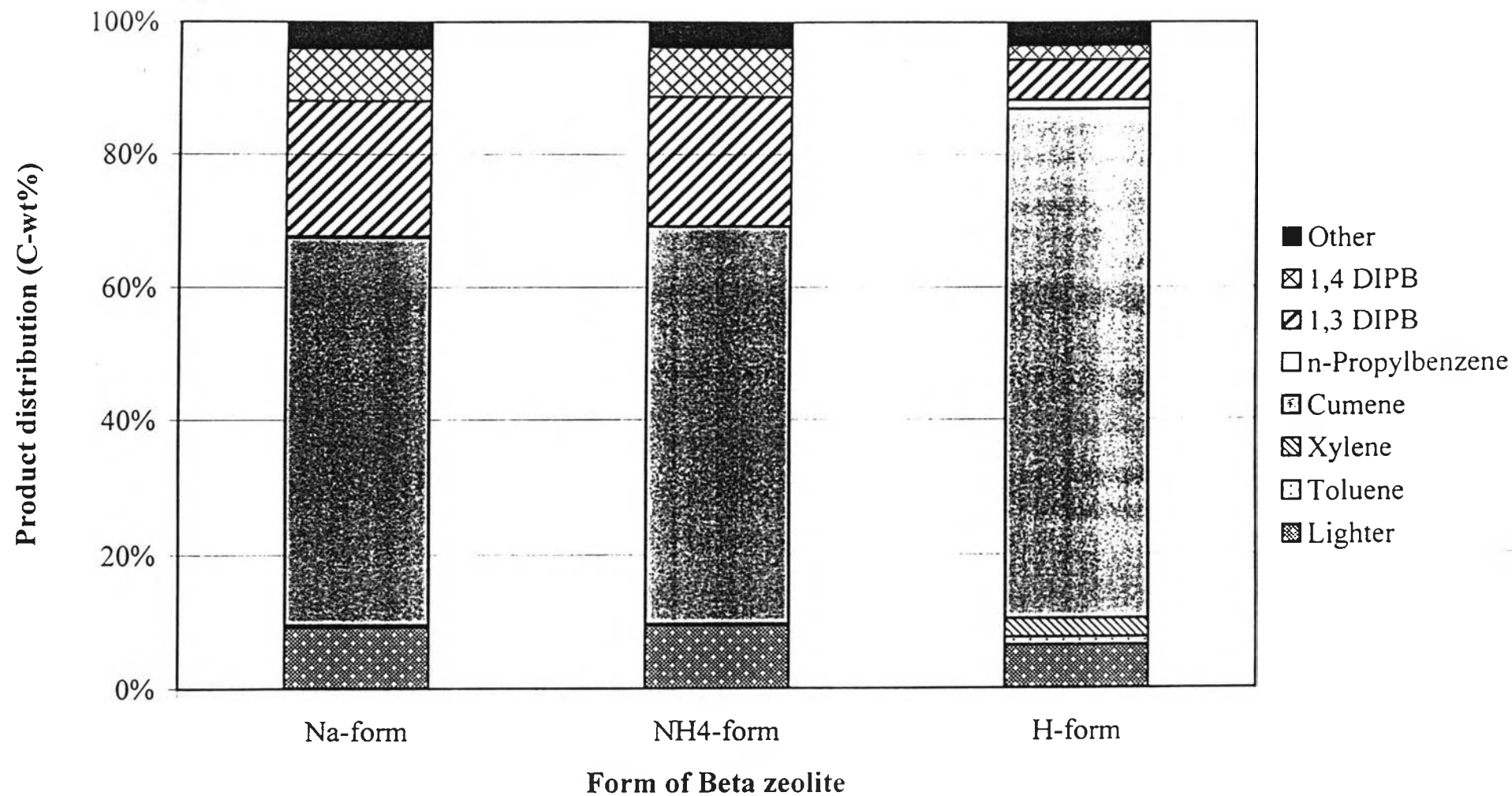
Figure 5.16 Effect of form of catalysts on product distribution.

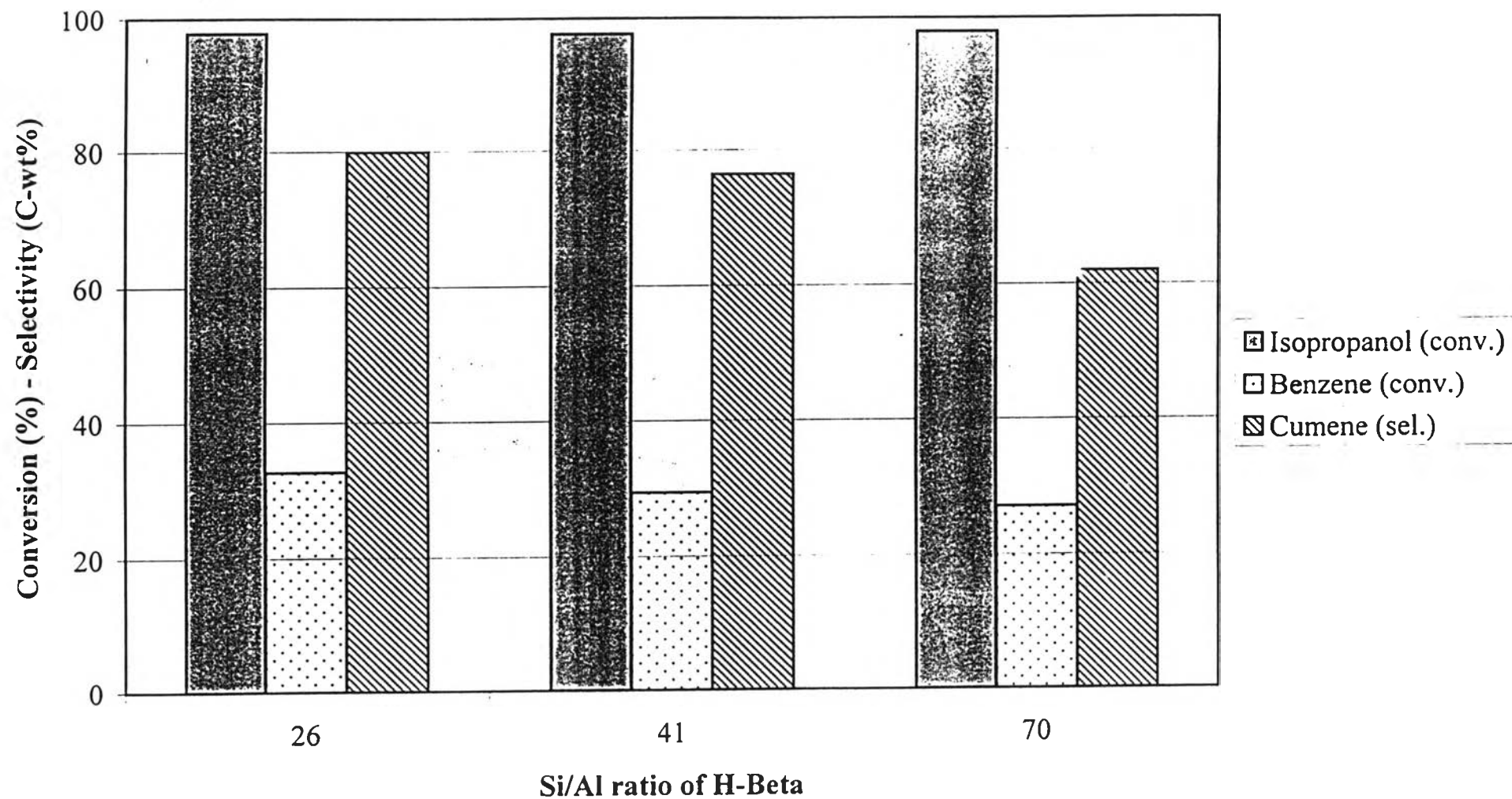Condition: Temperature 200°C, GHSV 3000 h^{-1}, TOS 40 min, H-Beta Si/Al = 41.

Figure 5.17 Effect of Si/Al ratio of H-Beta on conversion and selectivity.
Condition: Temperature 200°C, GHSV 3000 h^{-1}, TOS 40 min.
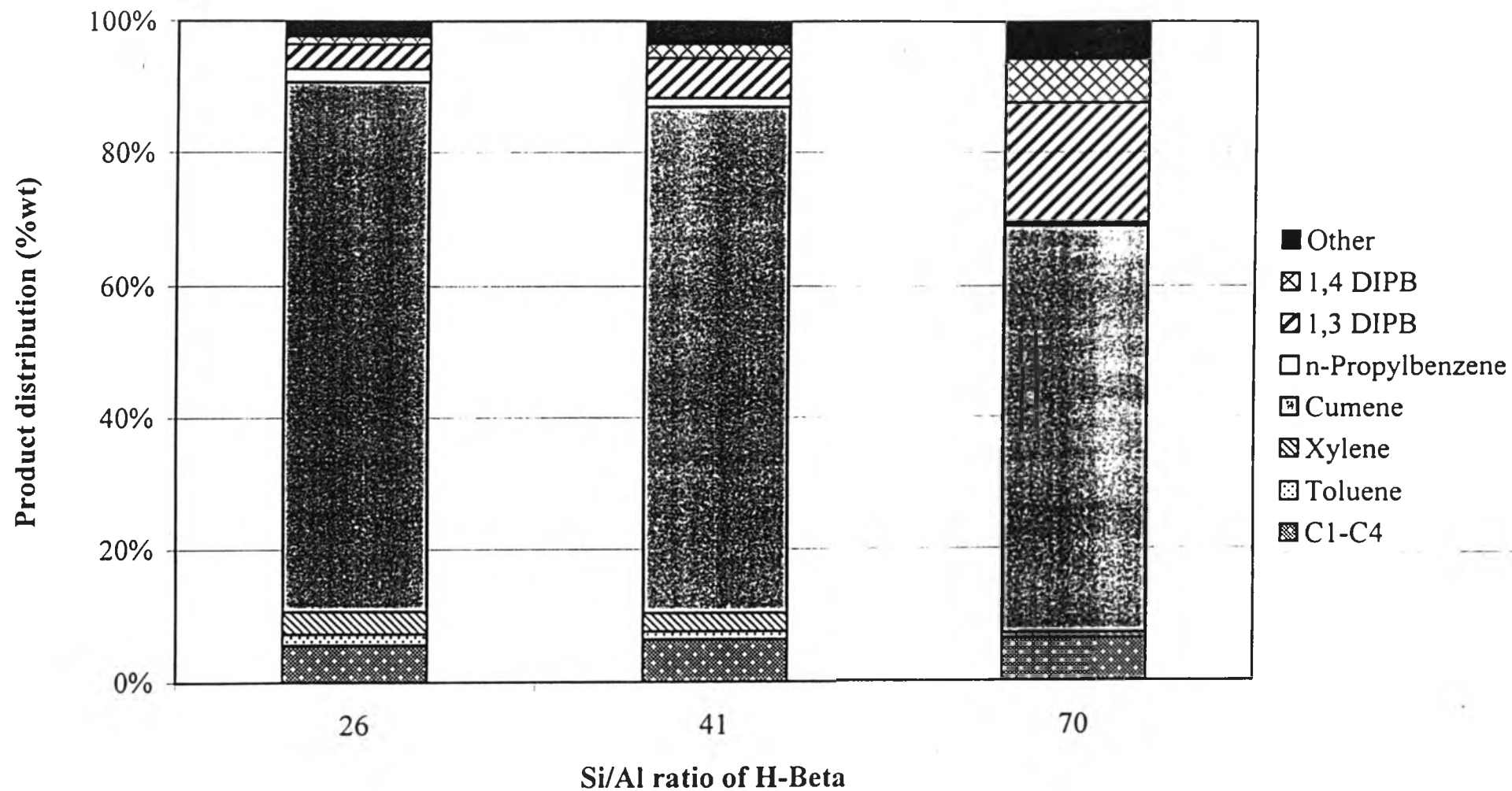
Figure 5.18 Effect of Si/Al ratio of H-Beta on product distribution.

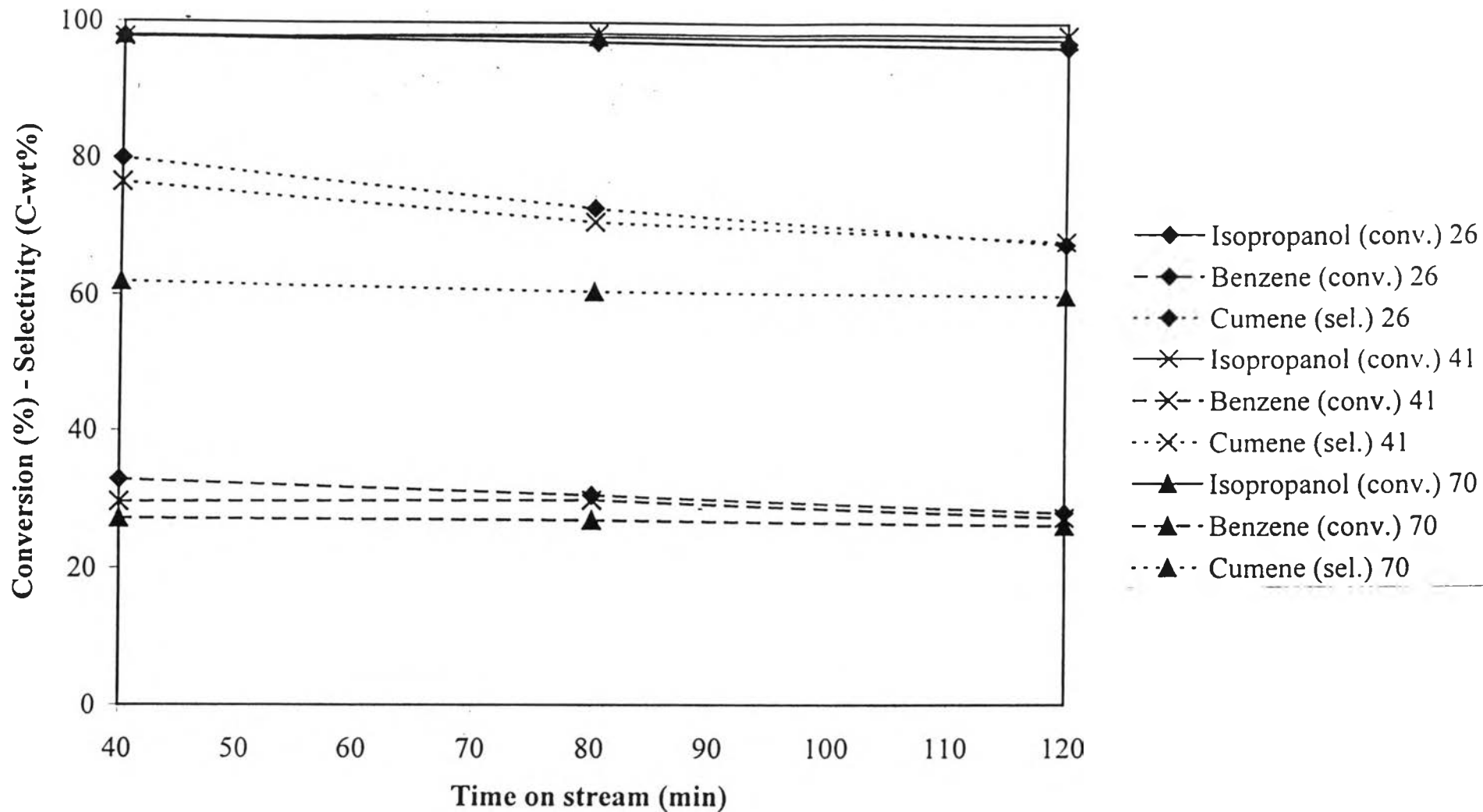Condition: Temperature $200^{\circ}C$, GHSV 3000 h^{-1}, TOS 40 min.

Figure 5.19 Compare effect of time-on-stream between H-Beta (26), H-Beta (41) and H-Beta (70). Condition: Temperature 200°C, GHSV 3000 h^{-1}.

5.2.6 Comparison of Catalysts

The catalytic activity and selectivity in alkylation of benzene with isopropanol over H-Beta, H-Y and H-ZSM-5 are compared in Figure 5.20. The reaction test was carried out at the optimum condition giving the highest yield (based on benzene conversion) for cumene of each catalyst. Commercial samples of H-Y and H-ZSM-5 were used as supplied by Tosoh Corporation and ALSI-PENTA ZEOLITE SM-55, respectively.

In all zeolites the conversion of isopropanol is more than 97%. The cumene selectivity is much higher for H-Beta compared to H-Y and H-ZSM-5. The faster deactivation was noticed over H-Y than H-Beta and H-ZSM-5. The cumene selectivity observed over H-Y (12-membered oxygen ring openings) is less than H-Beta (12-membered oxygen ring openings) due to the formation of side products such as triisopropylbenzene [9]. This seems to be reasonable because of the presence of supercages (diameter 12 Å) [9]. In contrast, H-Beta zeolite contains channels with access openings (7.6×6.4 Å and 5.5×5.5 Å) [24] that are only slightly larger than the size of benzene molecule. Therefore this catalyst should not permit the formation of those molecules with critical diameters that access significantly those of benzene. It has been found that a medium pore zeolite like H-ZSM-5 exhibited its highest yield for cumene lower than those obtained from Beta and Y zeolites, at higher temperature (275°C for H-ZSM-5 and 200°C for Beta and Y zeolites). The increase of n-propylbenzene formed in case of H-ZSM-5 is probably because of diffusion limitations, due to the constrained pores (10-membered oxygen ring openings) [9]. n-Propylbenzene is formed via bimolecular reaction between cumene and benzene [35]. The intersections of H-ZSM-5 zeolite are the most convenient geometry for this reaction [17].
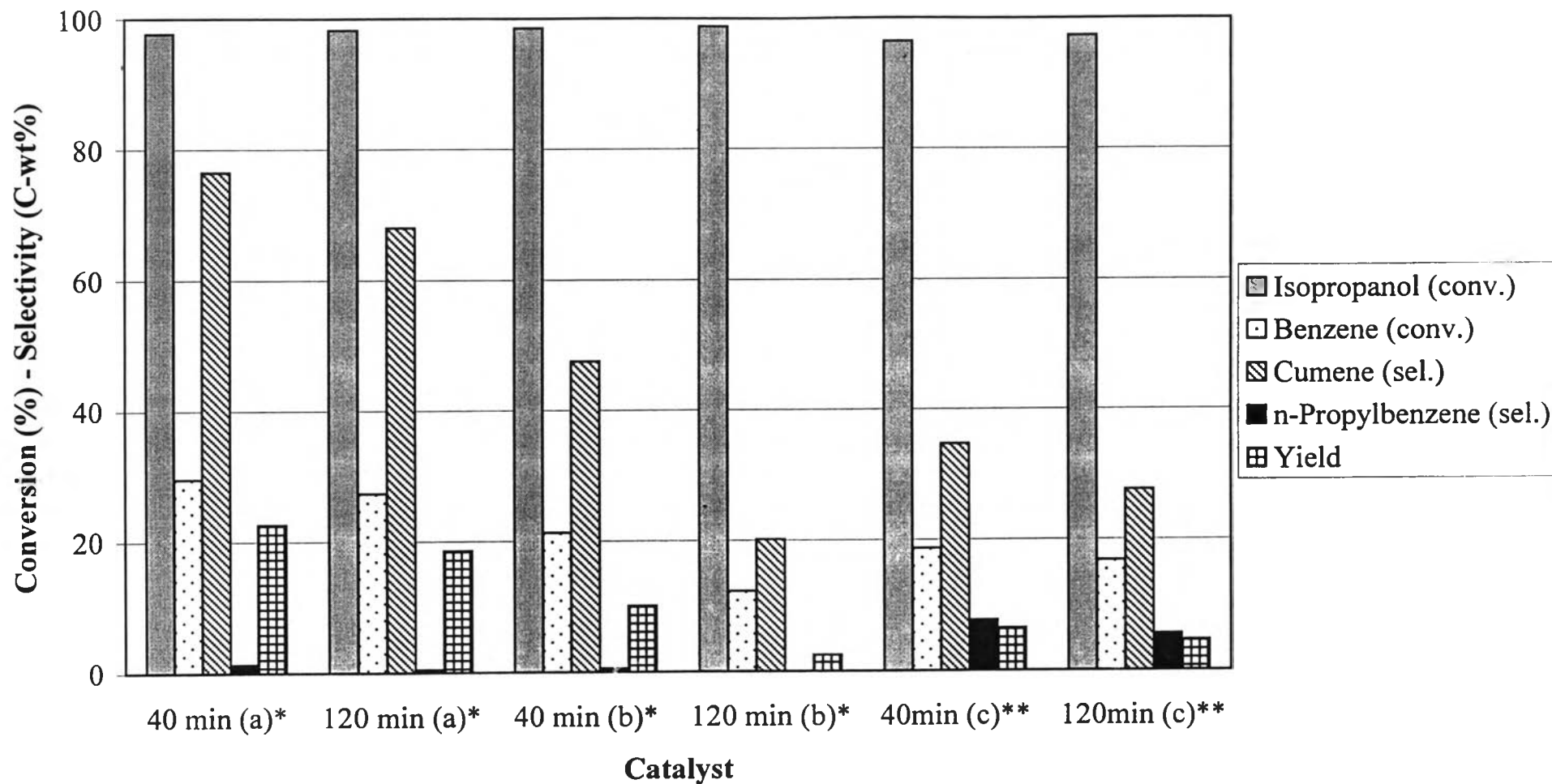
Figure 5.20 Comparison of catalysts (a) H-Beta (Si/Al = 41), (b) H-Y (Si/Al = 5.5) and (c) H-ZSM-5 (Si/Al = 55). Condition: GHSV 3000 h^{-1}, *Temperature 200°C, **Temperature 275°C.

5.2.7 Regeneration

Figures 5.21 and 5.22 show catalytic conversion and selectivity of the alkylation of benzene with isopropanol over fresh and regenerated catalyst at 200°C, GHSV 3000 h^{-1}, Si/Al = 41 observed after 40 minutes of TOS.

Regen1 represents the fresh catalyst after being used in the reaction for 6 hours, and then being regenerated at 550°C under air flow for 1 hour. Regen2 represents the Regen1, which is regenerated at the same condition after used in the reaction for 6 hours. From figure, it was found that H-Beta could be completely regenerated at regenerate condition used and give the catalytic performance as well as fresh catalyst.

5.2.8 The Effect of alkylating agent

The effect of an alkylating agent is shown in Figure 5.22. Isopropylation was carried out using propylene and isopropanol. The reaction was carried out at temperature 200°C, GHSV 3000 h^{-1}, TOS 40 and 180 min over H-Beta (Si/Al = 41). The faster deactivation is observed when propylene is used as an alkylating agent. The stronger adsorption of alkene on the active sites may be one of the reasons for the deactivation [17,33].
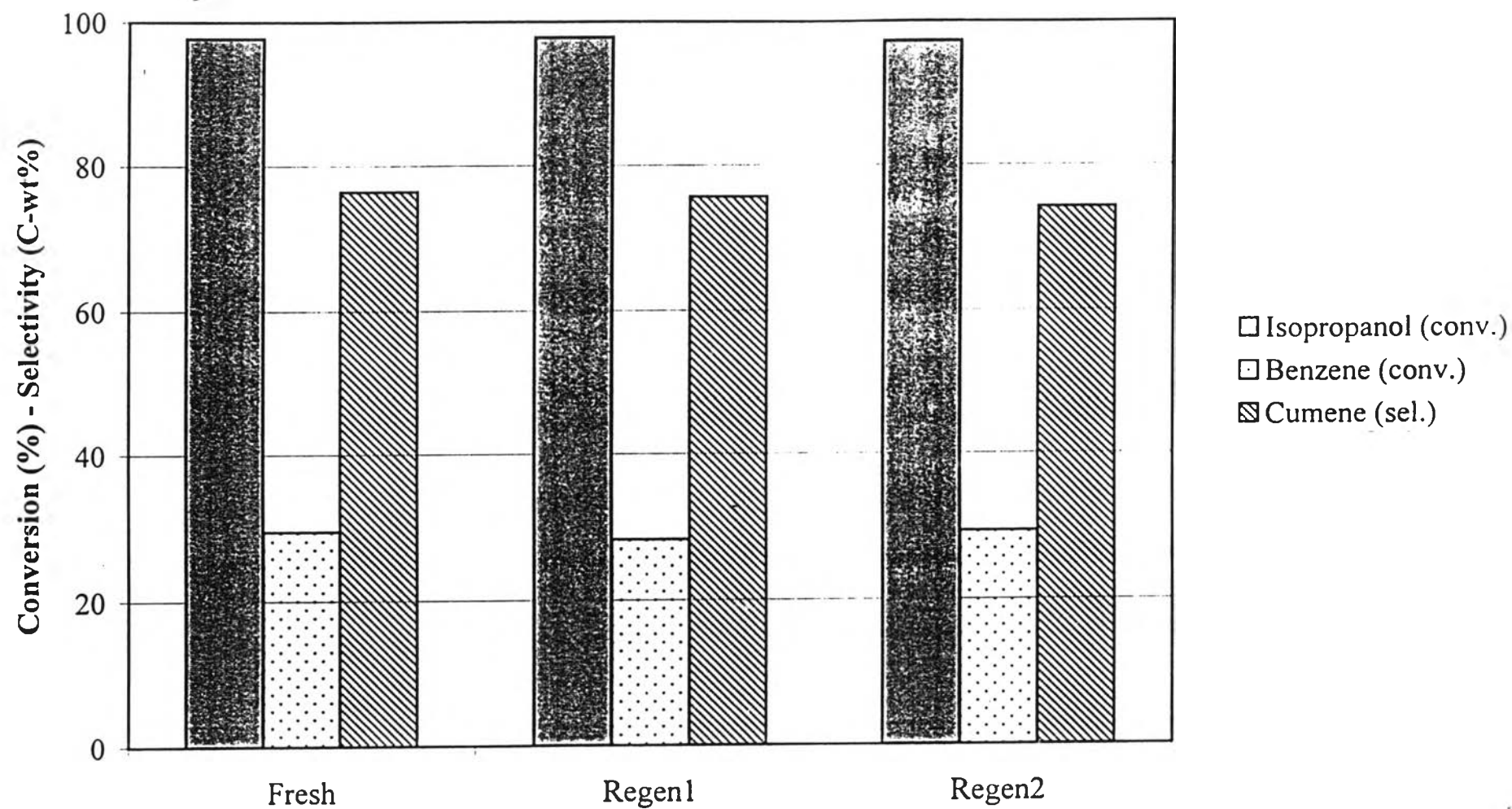
Figure 5.21 Effect of regenerated H-Beta on conversion and selectivity.
Condition: Temperature 200°C, GHSV 3000 h^{-1}, TOS 40 min.
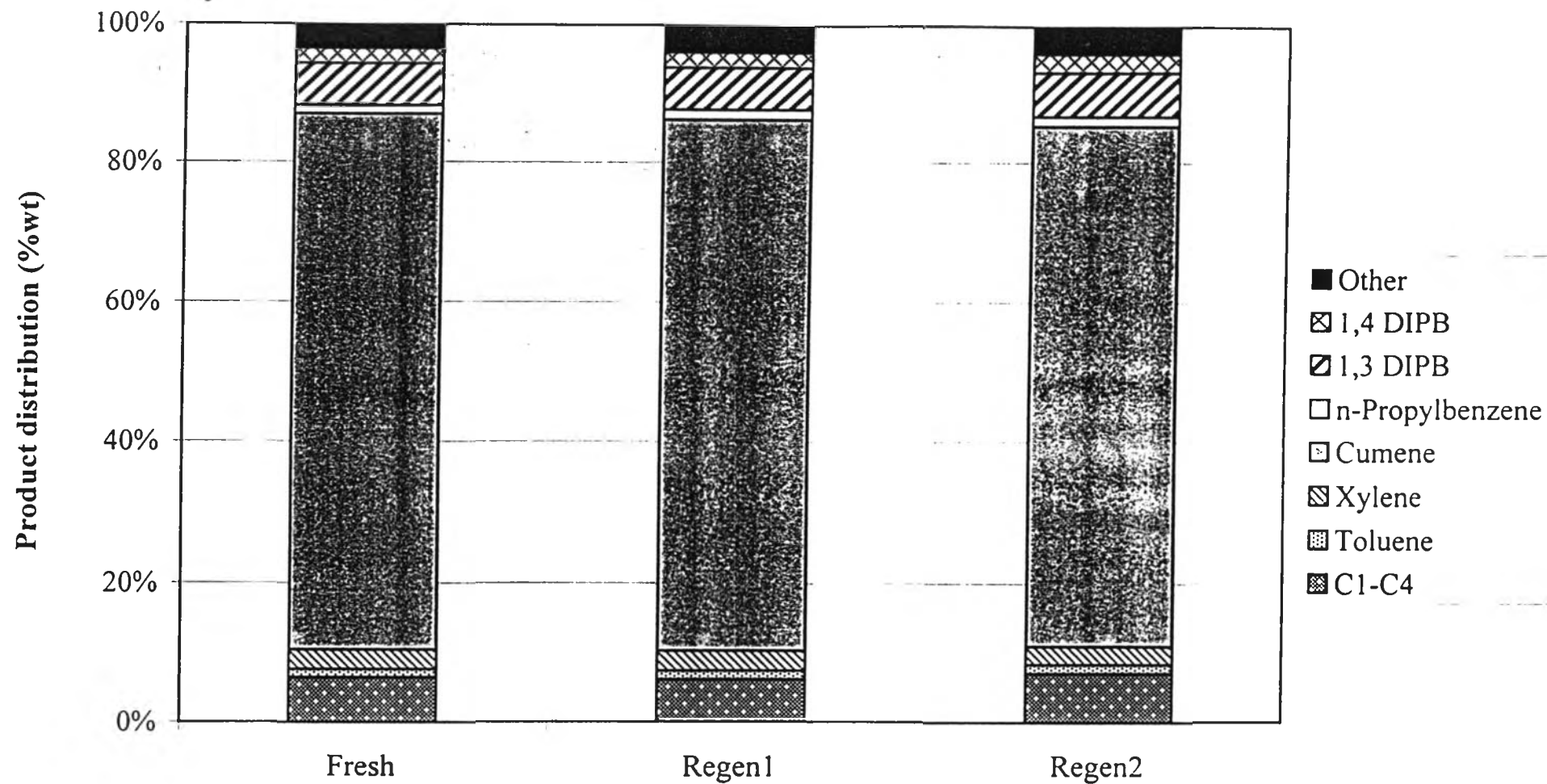
Figure 5.22 Effect of regenerated H-Beta on product distribution.

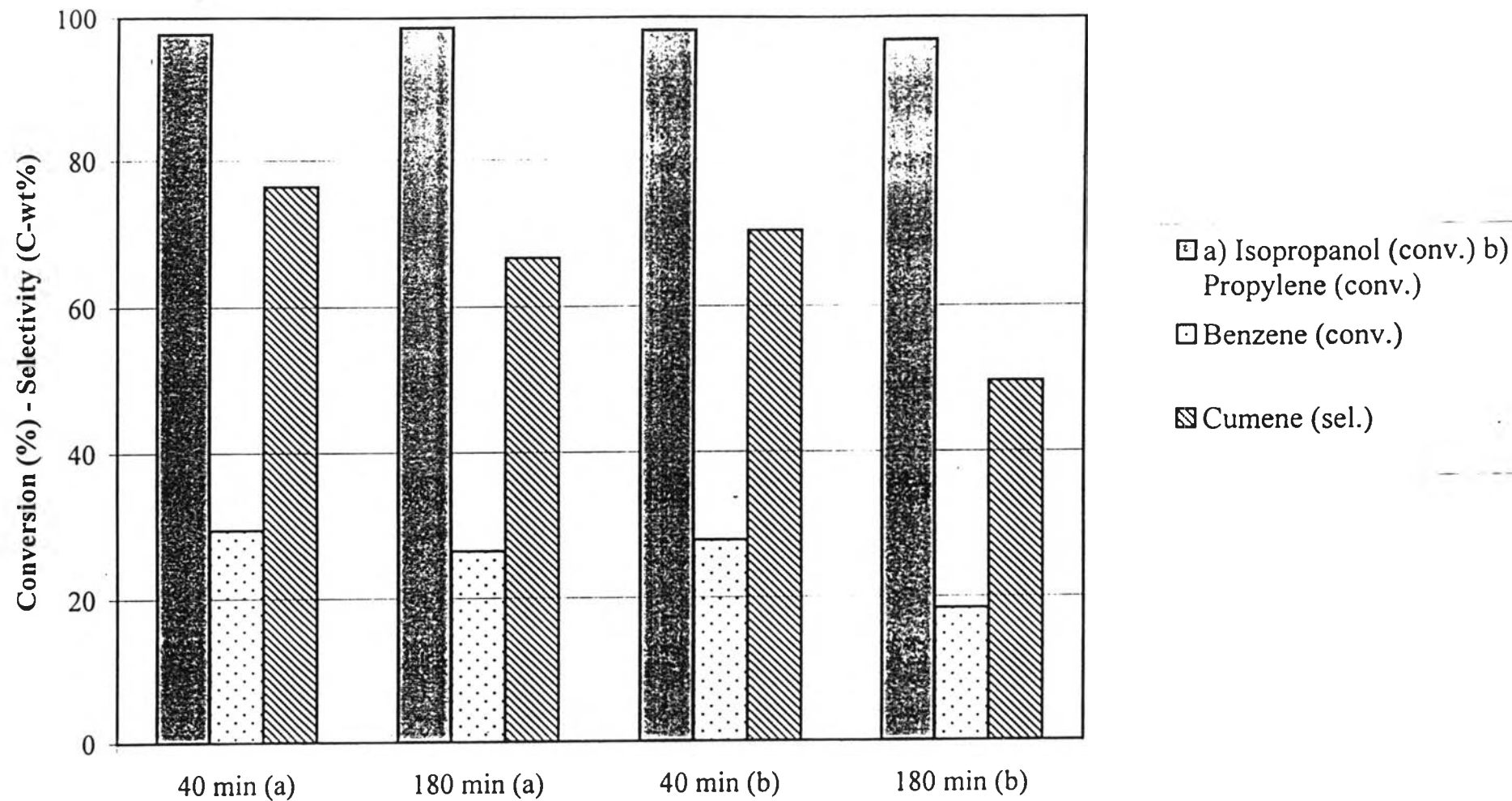Condition: Temperature 200°C, GHSV 3000 h⁻¹, TOS 40 min.

Figure 5.23 Effect of alkylating agent. (a) Isopropanol as alkylating agent (b) Propylene as alkylating agent
Condition: Temperature 200°C, GHSV 3000 h^{-1}, TOS 40 min.